



## Synthesis, Characterization And *In-Vitro* Studies On Chalcone Based Quinoxaline: *Acetylcholinesterase* Inhibition Through *In-Silico* Technique For Alzheimer's Disease

Venkatachalm T<sup>1\*</sup>, Manisha M<sup>2</sup>, Senthil Kumar N<sup>3</sup>.

<sup>1\*,2,3</sup>Department of pharmaceutical chemistry, JKKMRF-Annai J.K.K Sampoorani ammal college of pharmacy, Namakkal, Affiliated to The Tamil Nadu Dr.M.G.R. Medical University, Chennai, Tamil Nadu - 638183.

Email id: venkatmohana301108@gmail.com<sup>1</sup>, Phone number: +91 9843441716<sup>1</sup>

E mail id: manisha250799@gmail.com<sup>2</sup>, Phone number: +91 6374036954<sup>2</sup>

Email id : senthilkumarjkkm@gmail.com<sup>3</sup>, Phone number: +91 9842024640<sup>3</sup>.

**\*Corresponding author:** Venkatachalm T

Email id: venkatmohana301108@gmail.com<sup>1</sup>, Phone number: +91 9843441716\*

### Abstract

Inhibition of Acetylcholine esterase (AChE) to prevent the reduction of ACh level in Alzheimer's disease (AD) patients has been a popular strategy. Therapeutic applications of chalcones and Quinoxalines are becoming the attractive target due to its inherent diverse biological properties in recent times. In this study, virtual library was created containing 15 novel chalcone-quinoxaline hybrid derivatives using CHEMDRAW. Toxicity and ADME properties of those compounds were screened using admetSAR. 2D-QSAR *in-silico* models were developed to predict the activities of newly designed compounds before a decision is being made whether these compounds should be really synthesized and tested. In addition, docking studies had performed for newly designed compounds using PyRx software. 15 compounds were synthesized and characterized by IR, <sup>1</sup>H NMR, <sup>13</sup>C NMR and LC-MS. Then all compounds were tested for cell viability *in-vitro* MTT assay. Among the tested compounds, M2 and M4 were shown to be the most effective against the evaluated cell lines. In-depth, detailed investigations on *in-vivo* activity may be undertaken. The current study suggests that more research is needed for chalcone merged quinoxaline derivatives developed as a potent lead for Alzheimer's disease.

CC License  
CC-BY-NC-SA 4.0

**Key Words:** QSAR, Docking, chalcone, quinoxaline, Acetylcholine esterase Alzheimer's disease.

## 1. INTRODUCTION

Molecular hybridization (MH) is a strategy used for the design of new chemical entities by the fusion of two different chemotypes. This is an alternative to combination chemotherapy, where two or more drugs of different mechanisms of action were combined for the treatment [1, 2]. However, the simple combination chemotherapy has a high risk of drug-drug interaction [3]. The molecular hybridization is a rational design

of new ligands or prototypes based on the recognition of pharmacophoric sub-unities in the molecular structure of two or more known bioactive derivatives which, through the adequate fusion of these sub-unities, lead to the design of new hybrid architectures that maintain pre-selected characteristics of the original templates. Considering the use of known template substances, already evaluated concerning the physicochemical and pharmacological features, toxicity and mechanism of action, it is possible the generation of extensive chemical libraries, constituted by hundreds or even thousands of homologous molecular hybrids, bringing a high level of accumulated information, *e.g.* structural requirements, ligand-protein interaction mode, site ligand receptor interactions and quantitative structure-activity relationships, which tends to become faster and more efficient the development of new drugs [4,5]. On the other hand, if the degree of template-hybrid homology is either low or inexistent, massive screening of the generated chemical library should make the discovery of new lead-compounds [4]

### 1.1. CHALCONE AS CORE

Chalcones are recognized as a privileged scaffold for the incorporation of different molecules or pharmacophores with various activities. In addition to the biological activities for multitargeting mechanisms, hybrid molecules are also selected for other reasons, such as improving the solubility and oral bioavailability. A chalcone is a simple chemical scaffold of many naturally occurring compounds and has a widespread distribution in vegetables, fruits, teas, and other plants [6-10]. Chalcones, one of the main classes of flavonoids, are precursors of flavonoid and isoflavonoid biosynthesis. Chalcone compounds have a common chemical scaffold of 1,3-diaryl-2-propen-1-one, also known as chalconoid, that exists as *trans* and *cis* isomers, with the *trans* isomer being thermodynamically more stable [8,11]. *Trans* - Chalcone, a semisynthetic Chalcone with a simple structure, is the core of Chalcone compounds. The Chalcone family has attracted much interest not only from the synthetic and biosynthetic perspectives but also due to its broad interesting biological activities. Therapeutic applications of chalcones trace back thousands of years through the use of plants and herbs for the treatment of different medical disorders, such as cancer, inflammation, and diabetes. Several chalcone-based compounds have been approved for clinical use. For example, metochalcone was once marketed as a choleric drug, while sofalcone was previously used as an antiulcer and mucoprotective drug. Chalcones have been extensively studied, with many mini reviews published [12-27]. However, the accurate mechanisms of action for the wide-ranging biological activities of chalcones are still not well understood.

### 1.2 QUINOXALINE AS CORE

Nitrogen-containing heterocycles are promising compounds for the development of new drugs or novel potential lead molecules [28–31]. The quinoxaline scaffold, a bioisoster of quinoline and naphthalene, is one of the heterocycles currently attracting attention. Currently, there are several drugs containing a quinoxaline core unit such as echinomycin, levomycin and quinacillin (antibiotics), varenicline (nicotinic receptor agonist), brimonidine (eye drop), chloroquinoxaline sulfonamide (anticancer agents), and sulfaquinoxaline (used in veterinary medicine). Quinoxalines are becoming the attractive target for extensive research due to its inherent diverse biological properties. Various potential activities of the quinoxalines have been explored recently like antimicrobial agents, cytotoxic agents, anti-tubercular, anxiolytic, anti-HIV, anti-inflammatory, antioxidant, antileishmanial etc. In the recent year, 2,3-disubstituted quinoxalines reported to posse's significant potential against parasites, bacteria, fungi, and mycobacterium.

Chemically, quinoxaline is a low melting solid, purified by distillation, and a fraction of boiling point 108°-111/12mm has a melting point 29-30°C [32,33]. Quinoxalines are soluble in water, and produces monoquaternary salts when treated with quaternizing agents, like dimethyl sulfate and methyl p-toluene sulphonate. The quaternary salts of 2-alkylquinoxalines are unstable and converted into complex colored products by oxidation [32]. It is acidic with a pKa of 0.60 in water at 20°C, and nitration occurs only under forcing conditions (Conc. HNO<sub>3</sub>, Oleum, 90°C), resulting in the formation of two compounds: 5-nitroquinoxaline (1.5%) and 5,7-dinitroquinoxaline (24%) [33]. It's second pKa is 5.52 indicating that quinoxaline is significantly diprotonated in a strongly acidic medium.

### 1.3 ACETYLCHOLINESTRASE AS PRIMARY TARGET

Alzheimer's disease (AD), a progressive neurodegenerative disorder is a complex multifactorial disease characterized by formation and deposition of extracellular amyloid  $\beta$  (A $\beta$ ) plaques and intracellular neurofibrillary tangles (NFTs), oxidative stress, mitochondrial dysfunction and neuro-inflammation. The underlying mechanisms lead to neuronal loss with associated progressive decline in cognitive functions including memory loss. AD is the most common cause of dementia in elderly. Currently, estimated that 5.8

million Americans age 65 and older are living with Alzheimer's related dementia and this number is expected to rise to 13.8 million by 2050 [34]. AD was first observed by German clinical psychiatrist and neuroanatomist, Alois Alzheimer on November 26, 1901 while examining a patient Auguste Deter, 50-year-old woman who presented symptoms of sleep disorders, memory disturbance, and progressive confusion. After her death in 1906, postmortem of the brain showed senile plaques and neurofibrillary tangles. Later, the disease was coined as "Alzheimer's disease" [35]. Drug development for AD so far has mainly focused on cholinergic, beta amyloid hypothesis and tauopathy. Recently, the field has expanded to other pathologies including mitochondrial dysfunction and neuroinflammation [36]. Extensive research on drug discovery and development has led to FDA-approved drugs which include cholinesterase inhibitors such as donepezil (DPZ) [37–39], rivastigmine (RIV) [40–42], galantamine [43,44], and a partial N -methyl-D-aspartate (NMDA) antagonist, Memantine[45,46]. Unfortunately, these drugs can only manage the symptoms of AD for short-term and do not slow or stop the disease progression. Thus, a more effective therapeutic agents which can prevent progression or reverse the disease course is warranted.

Development of cholinesterase inhibitors is based on the cholinergic hypothesis [47]. According to the cholinergic hypothesis, first proposed by Peter Davies and A.J. Maloney in 1976 [48], neuronal synapses in AD patient have low levels of neurotransmitter, acetylcholine (ACh) accompanied by a decreased activity of choline acetyltransferase (ChAT). ACh is synthesized in cytoplasm of presynaptic cholinergic neurons from choline and acetyl coenzyme A (Acetyl-CoA) catalyzed by ChAT [49]. Once formed, it is transferred into synaptic vesicles. Exocytosis from presynaptic neuron upon depolarization releases ACh into synapses, which can bind with nicotinic or muscarinic receptors in postsynaptic neurons causing neurotransmission [50]. In synapses, ACh is primarily hydrolyzed by the enzyme called *acetylcholinesterase* into choline and acetic acid which switches off the cholinergic neurotransmission [51]. Reuptake of choline by presynaptic neurons for resynthesis of ACh completes the cycle [52]. Inhibition of AChE to prevent the reduction of ACh level in AD patients has been a popular strategy. Butyrylcholinesterase (BuChE, pseudocholinesterase) is another abundant cholinesterase and it differs from AChE with regards to substrate specificity. AChE is highly specific to ACh whereas BuChE favors butyrylcholine (BuCh) and several other cholinesters including Ach.

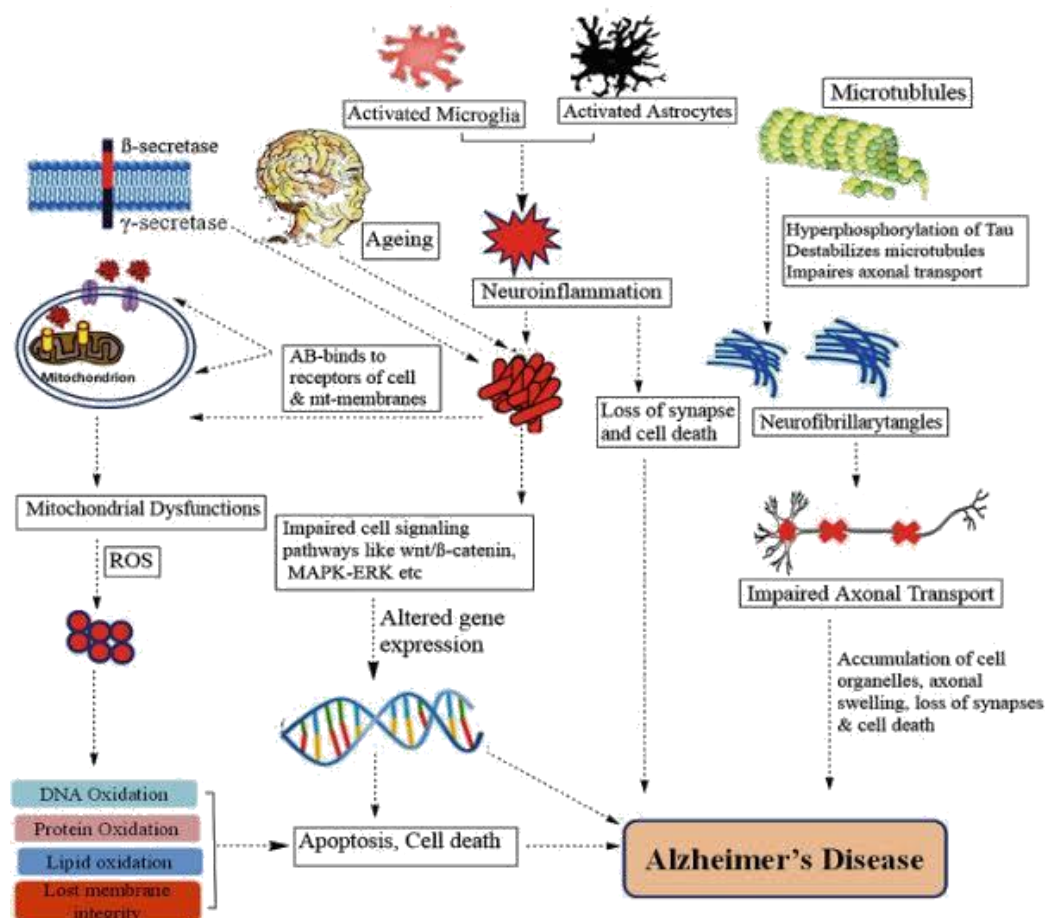


**Figure 1. Pathophysiology of Alzheimer's Disease**

## 2. MATERIALS AND METHOD

### 2.1 Reagents and Instrumentation

Oven dried glass wares were used to perform all the reactions. Procured reagents were of analytical grade and solvents of laboratory grade and purified as necessary according to techniques mentioned in Vogel's Textbook of Practical Organic Chemistry. In an open glass capillary tubes using Veego VMP-1 apparatus, melting points have been determined in °C and are uncorrected. Ascending TLC on precoated silica-gel plates (MERCK 6 F254) visualized under UV light was utilized to routinely monitor the progress and purity of the synthesized compounds. Solvents used during TLC are n-hexane, ethyl acetate, methanol, petroleum ether, chloroform and dichloromethane. The Infrared Spectra was plotted by Perkin-Elmer Fourier Transform-Infrared Spectrometer and in reciprocal centimetres the band positions are noted. Nuclear magnetic spectra (<sup>1</sup>H NMR) were obtained from Bruker DRX-300 (500 MHz FT-NMR) spectrophotometer using DMSO as solvent with TMS as the internal standard <sup>13</sup>C NMR have been recorded utilizing Bruker with Dimethyl sulphoxide as solvent. Shimadzu LC-MS was employed to record Mass Spectra.

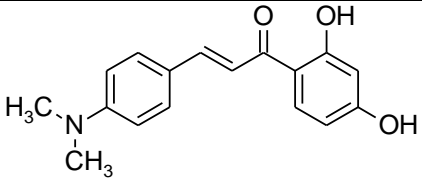
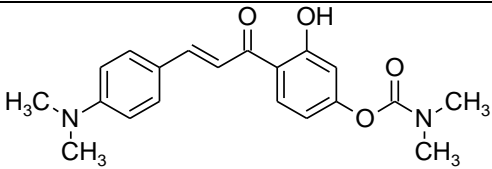
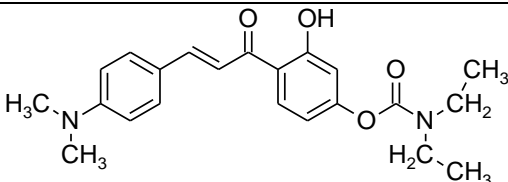
### 2.2 2D-QSAR

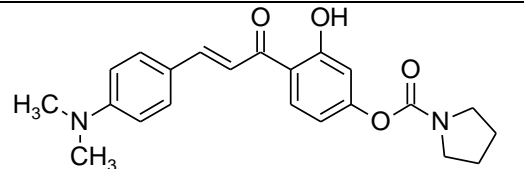
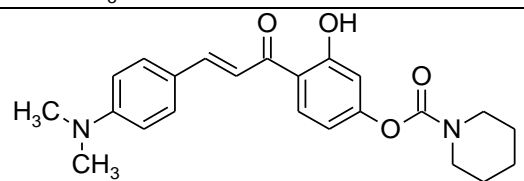
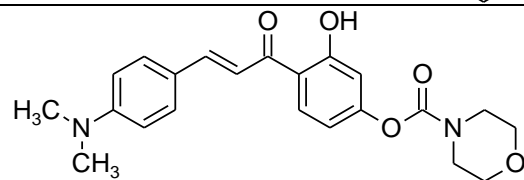
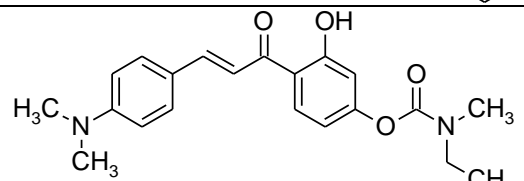
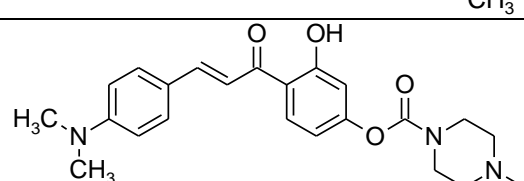
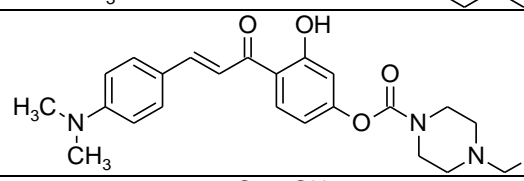
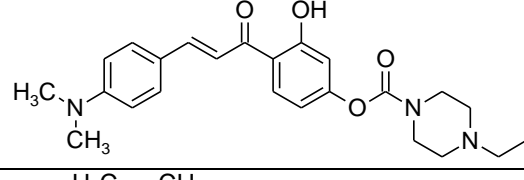
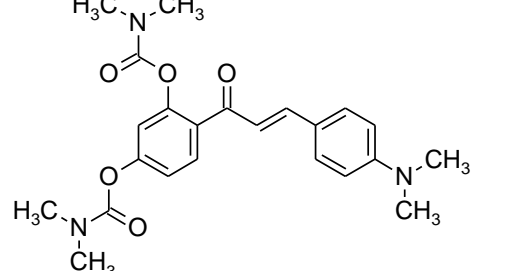
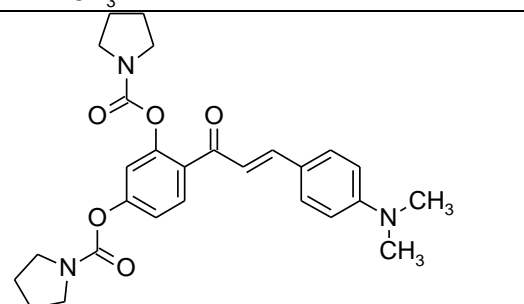
The QSAR studies are useful tools for screening chemicals, especially in early stages of the drug discovery process, which have provided no experimental data. If these are properly developed and rigorously validated, they become outstanding tools to evaluate only those that are most promising. As the first preliminary step of a QSAR model development, relevant chemogenomics data are collected from databases and the literature. Then, chemical descriptors are calculated on different levels of representation of molecular structure, ranging from 1D to nD, and then correlated with the biological property using machine learning techniques. Once developed and validated, QSAR models are applied to predict the biological property of novel compounds. Although the experimental testing of computational hits is not an inherent part of QSAR methodology, it is highly desired and should be performed as an ultimate validation of developed models. In the last two decades, QSAR models have been successfully used to search new molecular entities, correlating significant structural properties with the biological activity of a compound. In this sense, our research group have obtained several remarkable results in the identification/selection of new molecular entities with potential action against different targets.

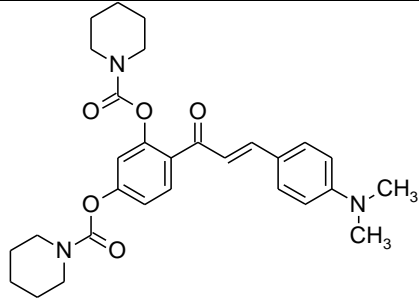
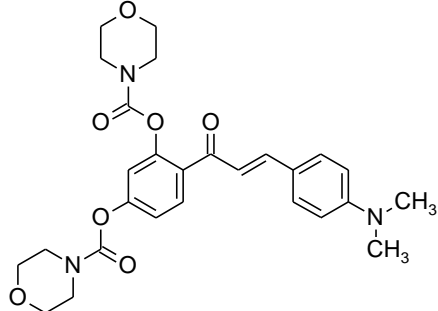
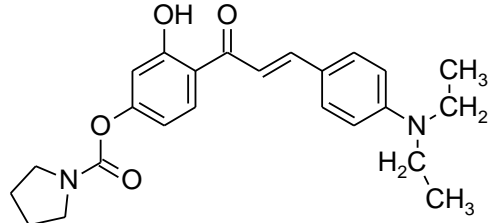
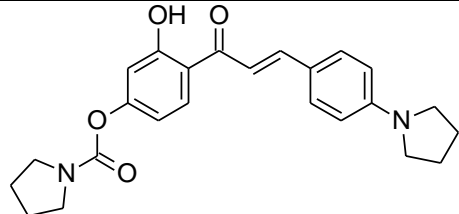
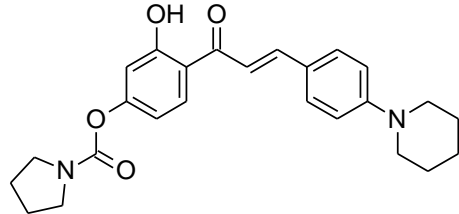
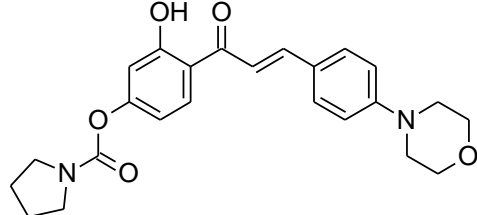
The main objective of the present study was to obtain a statistically significant model to predict the AChE inhibition and to identify new hits, which could be potential anti-Alzheimer agents. We used the QSAR-INSUBRIA (QSARINS) software to develop a Multiple Linear Regression (MLR) model to identify the potentially new inhibitors.

### 2.3 Data set

A dataset of 18 compounds were used in this experimental work selected from various reported literature. All the chemical structures along with their biological activity were based on Chalcone derivatives as Ache inhibitors. Table 1 shows the data set for the study.

Compound code	Structure	IC50	pIC50
1		78.21	-1.89326
2		32.62	-1.51348
3		17.21	-1.23578

4		4.19	-0.69108
5		6.9	-0.83885
6		8.01	-0.90363
7		14.33	-1.15625
8		11.94	-1.077
9		8.62	-0.93551
10		21.43	-1.33102
11		100	-2
12		30.01	-1.47727

13		32.44	-1.51108
14		18.01	-1.7635
15		11.74	-1.06967
16		14.06	-1.14799
17		10.62	-1.02612
18		63.5	-1.80277

## 2.4Compound library

About 15 compounds were designed using ChemDraw software (**figure 1**). ChemDraw is a molecule editor first developed in 1985 by David A. Evans and Stewart Rubenstein [70] (later by the cheminformatics company Cambridge Soft). The company was sold to PerkinElmer in the year 2011 [71]. The designed compounds of Chalcone and quinoxaline hybrid shown in figure 2.

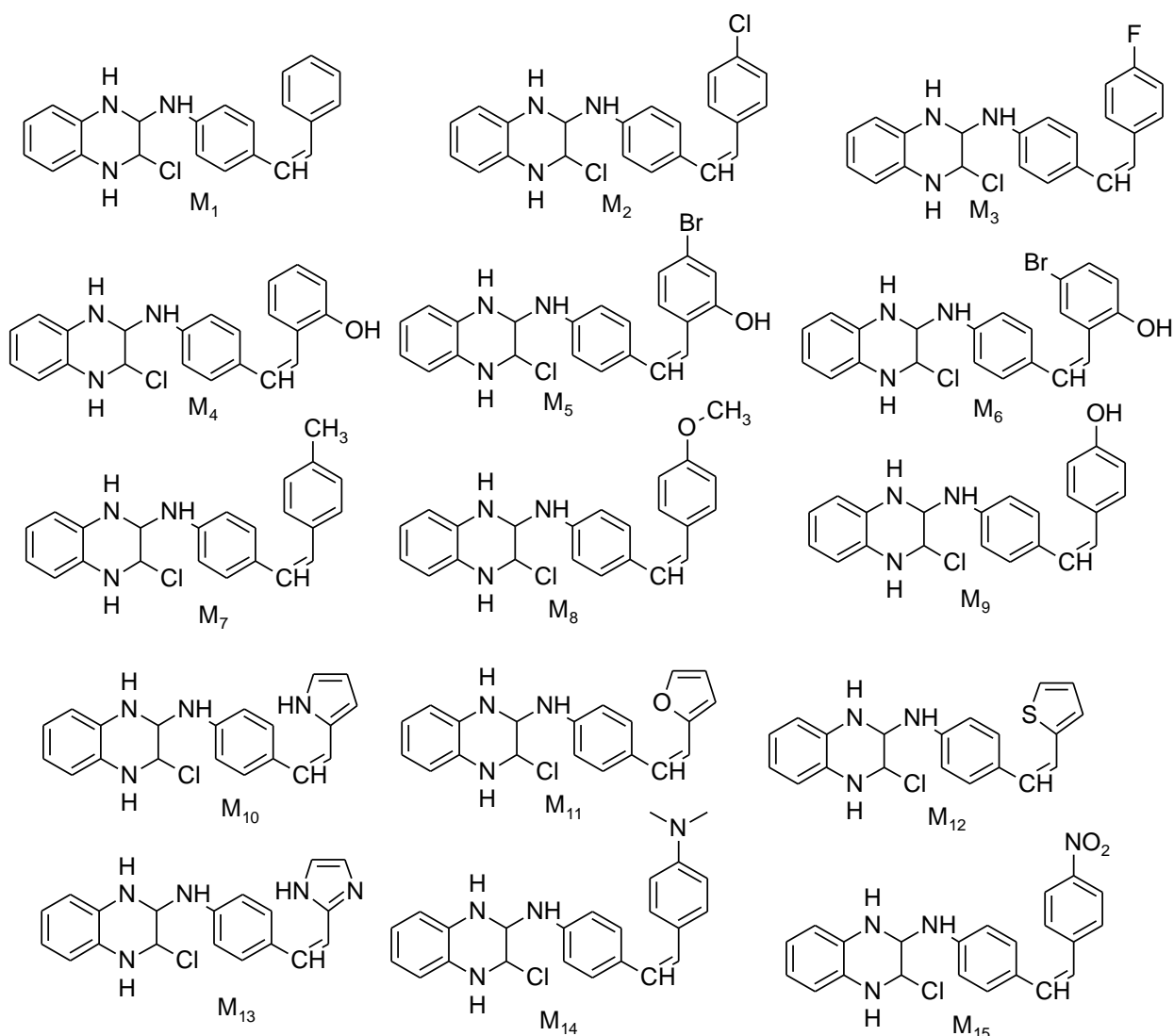


**Figure 2:** Newly designed derivatives

## 2.5 *In-silico* molecular docking studies

### 2.5.1 Devices and materials

In the molecular scenario in the modern drug design, the docking is commonly used to understand the interaction between the target ligand-receptor and the target lead molecule's binding orientation with its protein receptor and is quite frequently used to detect the associations between the target components. The research work was done *in-silico* by utilizing bioinformatics tools. Also, we utilize some of the offline programming's like protein data bank (PDB) [www.rcsb.org/pdb](http://www.rcsb.org/pdb), PubChem database, Marvin sketch. The molecular docking studies were carried out through PyRx docking software.

### 2.5.2 Preparation of protein

By utilizing the offline program protein data bank (PDB), we take the AChE (PDB ID: 4E8Y) was obtained from PDB website. From the protein we removed the crystal water, followed by the addition of missing hydrogens, protonation, ionization, energy minimization. The SPDBV (swiss protein data bank viewer) force field was applied for energy minimization. Prepared protein is validated by utilizing the Ramachandran plot.

### 2.5.3 Identification of active sites

Identification of active amino acid present in the protein is detected by using Protein-ligand interaction profile (PLIP) <https://plip-tool.biotec.tu-dresden.de/plipweb/plip/index> online tool in google. From this, we found the active amino acid present in the protein.

### 2.5.4 Preparation of Ligands

By utilizing the Marvin sketch tool, the designed molecules are sketched in two and three-dimensional structures. After designed molecule, the structure was optimized in 3D optimization in Marvin sketch and saved as a pdb format.

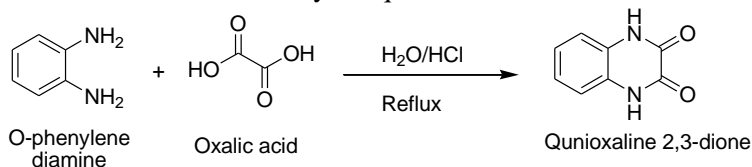
## 2.5.5 Molecular Docking

We used PyRx virtual screening tool because it showed higher docking accuracy than other stages of the docking products (MVD: 87%, Glide: 82%, Surflex: 75%, FlexX: 58%) in the market coordinates in PDB format. Non-polar hydrogen atoms were removed from the receptor file and their partial charges were added to the corresponding carbon atoms. Molecular docking was performed using Molecular docking engine of PyRx software. The binding site was defined as a spherical region which encompasses all protein atoms within 15.0 Å of bound crystallographic ligand atom. Default settings were used for all the calculations. Docking was performed using a grid resolution.

## 2.6 Chemistry

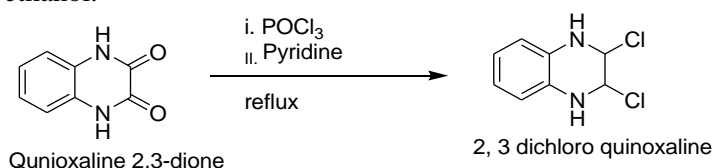
### 2.6.1 Step 1. Synthesis of 1,4-Dihydro-quinoxaline-2,3-dione

Oxalic acid (0.238 mole, 30 g) was dissolved in H<sub>2</sub>O (100 ml), followed by addition of concentrated hydrochloric acid 4.5 ml, then *O*-phenylenediamine (0.204 mole, 22 g) was added. The reaction was refluxed for 20 min. Then it was cooled by addition of ice. The solid was filtered, washed with water, recrystallized from ethanol until 1,4-Dihydro-quinoxaline-2,3-dione was obtained.



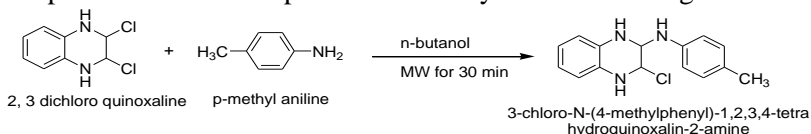
### 2.6.2 Step 2. Synthesis of 2, 3 dichloroquinoxaline

1,4-dihydro-quinoxaline-2,3-dione (1)(0.05 mole, 8.1 g), POCl<sub>3</sub> (0.08 mole, 7.35 ml) and pyridine (0.05 mole, 9.65 ml) was refluxed for 5 hrs. The mixture was allowed to cool, and then poured into crushed ice. The precipitate was filtered and washed with water. 2,3-Dichloro-quinoxaline was recrystallized from ethanol.



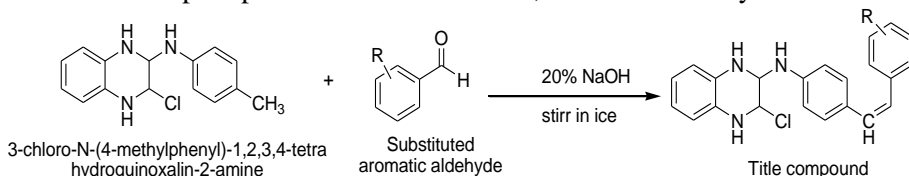
### 2.6.3 Step 3. Synthesis of 3-chloro-N-(4-methylphenyl)-1,2,3,4-tetra hydroquinoxalin-2-amine

2,3-dichloroquinoxaline (0.01mole) and *p*-methyl aniline (0.01mole) was added in *n*-butanol (2mL). It was subjected to irradiation in microwave at 130°C for 30 min. Reaction mixture was allowed to cool at room temperature. The crude product was recrystallization using ethanol.



### 2.6.4 Step 4. General procedure for synthesis of quinoxalin based chalcone derivatives

The product obtained from step.3 (0.01mole) was added to substituted benzaldehyde (0.01mole) in ethanol solvent. The mixture was stirred in ice bath using magnetic stirrer. Then add 10ml of 2N sodium hydroxide and stir for 30min. It is kept undisturbed overnight. The product is neutralized with hydrochloric acid in cold condition. The precipitate obtained is filtered, washed and recrystallized from ethanol



## 2.7 MTT assay

### 2.7.1 Cell culture

Human SH-SY5Y neuroblastoma cells were obtained from Sigma Aldrich and cultured in DMEM supplemented with 10% foetal bovine serum (FBS) at 37 °C in an environment humidified with 5.0% CO<sub>2</sub>. At 80% confluence, the experiments were conducted.

### 2.7.2 Determination of cell viability

Cell viability was evaluated using a MTT assay, as previously described, with slight modifications. The exam was conducted with three duplicates. Fresh medium (100 µL) with 10% FBS was added to 96-well plates with 2.0 x 10<sup>4</sup> cells per well. The cells were pretreated with five different dosages of test compounds (25, 50, 100, 250, and 500 µg/mL, solubilized in DMEM with 10% FBS) for two hours after stabilizing for 24 hours. After a 2-hour interval, the treatment was combined with 10 µM Aβ<sub>25-35</sub> and incubated for another 24 hours at 37.0°C with 5.0% CO<sub>2</sub>. The solvent control condition used in the statistical analysis was DMEM + 10% FBS. Following the treatment period, take out the culture medium and fill each well with 100 µL of MTT (500 µg/mL). Next, the plates were incubated for four hours. After removing the MTT solution, 100 µL of DMSO was added to each well in order to dissolve the dark blue crystals. After shaking the plates for a few minutes, a Thermo Plate scanner operating at 540 nm was used to scan the plates. Data were examined and presented in percentage terms in relation to the control group.

## 3. RESULTS AND DISCUSSION

### 4. 3.1 2D – QSAR

#### 2.8 Model Information and Interpretation

The resultant QSAR model for *acetylcholinesterase* inhibitors shows that five descriptors are involved in predicting the activity. With the criteria of all above mentioned, Model 1 is chosen for discussion. Experimental, predicted activities, leverage values of the model 2 and their residues are shown in **Table 2**.

**Model 1 = -12.6584 + 94.513 (AATSC3e) + 3.6902 (MATS6m) + 0.9277 (BCUTp-1) - 0.0906 (C1SP3) + 2.2487 (IC1).**

R<sup>2</sup>: 0.9201 R<sup>2</sup><sub>adj</sub>: 0.9086 R<sup>2</sup>-R<sup>2</sup><sub>adj</sub>: 0.0114 LOF: 0.0774

K<sub>xx</sub>: 0.3731 Delta K: 0.0529 RMSE tr: 0.2103 MAE tr: 0.1566

RSS tr: 1.8132 CCC tr: 0.9584 s: 0.2276 F: 80.5572

In this model 1, 1 compound were taken as training set and 5 compounds as the test set. The correlation coefficient value (r<sup>2</sup> value) of the model was 0.9201 which is merely equal to one. This manifests to be the best fit of the model. R<sup>2</sup><sub>adj</sub> determines the convenience for the addition of a new descriptor to the model. The difference between the R<sup>2</sup>-R<sup>2</sup><sub>adj</sub> must be lower to satisfy. The R<sup>2</sup>-R<sup>2</sup><sub>adj</sub> value is 0.0114 which is lower and satisfied. The absence of overfitting of the model is confirmed by the low value of Friedman's lack of fit (LOF). The LOF value in model 1 was 0.0774 and it is lower. The delta K value was positive (Delta K = 0.0529) which shows a good correlation between the biological activity and the descriptors. The quality of the model was confirmed by obtaining mean absolute error (MAE) and standard deviation (s) of estimate. The model shows MAE and s value as 0.1566 and 0.2276 respectively. This shows the good quality of the model. Therefore, AATSC3e, MATS6m, BCUTp-1, C1SP3, and IC1 are the descriptors shown best fit of the model. AATSC3e, MATS6m, BCUTp-1, IC1 showed a positive contribution, and C1SP3 showed a negative contribution in the generated model 1. Model 1 is analyzed for outliers by residual calculation. The compounds with higher values of residuals are considered as the outliers. To improve the quality of the model, residual compounds 1, 14, 18, are excluded and executed for further model prediction.

#### Model 2

**Model 2 = -7.4294 + 5.0435 (AATS0p) - 28.2950 (AATSC8e) + 0.9323 (GATS5e) - 2.0940 (VE1\_Dt) - 0.0621 (ZMIC3).**

R<sup>2</sup>: 0.9398 R<sup>2</sup><sub>adj</sub>: 0.9290 R<sup>2</sup>-R<sup>2</sup><sub>adj</sub>: 0.0108 LOF: 0.0710

K<sub>xx</sub>: 0.3746 Delta K: 0.0968 RMSE tr: 0.1880 MAE tr: 0.1472

RSS tr: 1.2023 CCC tr: 0.9689 s: 0.2072 F: 87.3504

After removing the outliers from model 1, model 2 was generated. In this model 2, 14 compounds were taken as a training set and 5 compounds as the test set. The r<sup>2</sup> value of model 2 increase from 0.9201 to 0.9398. It shows the best fitting of the model when compared to model 1. R<sup>2</sup><sub>adj</sub> is 0.9290 which is merely equal to R<sup>2</sup>. Friedman lack of fit (LOF) value is 0.0710 that makes the model fit with the activity in a stable manner. The quality of model 2 is also improved when compared to model 1. Mean Average Error (MAE) value (0.1472) and Standard Error of Estimate (s) (0.2072) values were reduced in model 2 that signifying the reduction in

the errors. The Concordance Correlation Coefficient (CCC) value is 0.9689 that is greater than 0.95 states the model to be substantial. In addition, the Delta K value is 0.0968 that is positive shows a better correlation between biological activity and the descriptors. In this model, the descriptors like AATS0p, GATS5E showed positive contributions, and AATSC8e, VE1\_Dt, and ZMIC3 showed negative contributions. Based upon the residual calculation for model 2, there is no outlier found in this model 2. Therefore, model 2 was the best of all the models generated by the software

**Table 2. Experimental, predicted activities, leverage values of the model 2 and their residues**

Com No	Status	Exp. Endpoint	Pred. By model eq.	Pred.mod. eq.res.	Pred. Loo	Pred. Loo res.	Hat i/i (h*=0.5 294)	Std.pred.m od.eq. Res.	Std.pred.l oo res.
2	Training	-1.6124	-1.5143	0.03971	-1.4648	0.0486	0.1039	0.2222	0.2479
3	Training	-1.2358	-1.3387	-0.1029	-1.3792	-0.1434	0.2825	-0.5863	-0.8171
4	Training	-0.6911	-0.782	-0.0909	-0.8006	-0.1095	0.1696	-0.4816	-0.58
5	Training	-0.8389	-0.8211	0.0178	-0.8173	0.0215	0.1732	0.0945	0.1142
6	Training	-0.9036	-1.0698	-0.1662	-1.1041	-0.2005	0.1711	-0.8809	-1.0627
7	Training	-1.1563	-1.2829	-0.1266	-1.3094	-0.1532	0.1735	-0.672	-0.8131
8	Test	-1.077	-1.032	0.045	-	-	0.2224	0.2463	0.2463
9	Test	-0.9355	-0.9764	-0.0409	-0.9858	-0.0503	0.1866	-0.2188	-0.2689
10	Training	-1.331	-1.0627	0.2683	-1.0482	0.2828	0.0514	1.3293	1.4014
11	Training	-2	-2.2611	-0.2611	-2.3844	-0.3844	0.3207	-1.5289	-2.2509
12	Training	-1.4774	-1.4173	0.0601	-1.3862	0.0912	0.3408	0.3572	0.5418
13	Training	-1.5111	-1.4495	0.0616	-1.4067	0.1043	0.4097	0.3868	0.6554
14	Test	-1.0697	-0.7925	0.2772	-	-	0.2473	1.5419	1.5419
15	Training	-1.148	-1.2208	-0.0728	-1.2295	-0.0815	0.1066	-0.3716	-0.416
16	Test	-1.0261	-1.2876	-0.2615	-1.3255	-0.2994	0.1267	-1.3502	-1.5461
17	Training	-1.8028	-1.3343	0.4685	-1.2771	0.5256	0.1087	2.3948	2.6868
18	Training	-1.5111	-1.4495	0.0616	-1.4067	0.1043	0.4097	0.3868	0.6554

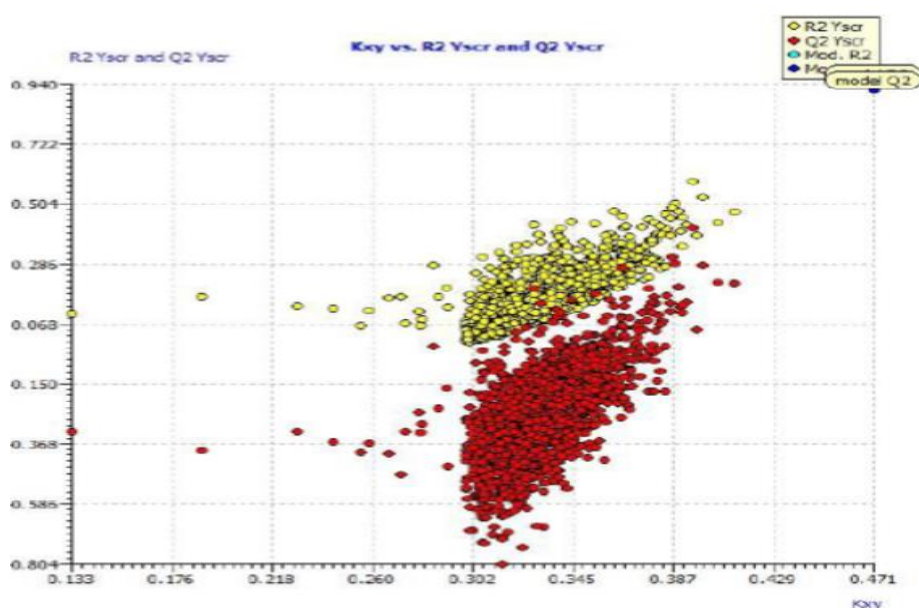


**Figure 3:** Plot for the Y-scrambling for the model 2.

## 2.9Molecular docking

The molecular docking studies for the designed compounds were carried out through PyRx molecular docking software to determine the free energy binding towards targeted enzymes. The docking pose for the ligand enzyme interaction was visualized with discovery studio. The binding free energy for all the ligands was tabulated in table. From the results it clearly shows that, all the compounds have promising interaction with targeted enzyme AChE. The interaction is mainly due to the presence of lipophilic factor of aromatic heterocyclic ring. From the docking results, compound M2 (8.7 kcal/mol) shows highest binding affinity toward AChE enzyme compared to standard drug donepezil. This compound produced one conventional hydrogen bonds between NH of quinoxaline moiety with residues of Asn 233. The following amino acids such as Thr238, Val239, Gly240, Pro410, Trp 532, and Leu536 are interact with ligand through hydrophobic bond. These interactions due to the aromatic character of ligands. The remaining the entire studied compound shows good to moderate binding affinities to the selected enzymes. These amino acids have been

repeatedly implicated during ligand interaction with the AChE enzyme and also play important role in the inhibition of the ligand-binding domain of AChE inhibitors. These non-covalent interactions, van der Waals, columbic interaction,  $\pi$ - $\pi$  interaction, and hydrogen interaction, are shown in **Figure 4 to 10**. The table 3 shows the binding energy of studied compounds. Based on the docking score the following derivatives like M2, M3, M4, M5, M6, M7, M8, M13, M14 and M15 are selected for the conventional synthesis and it was further evaluated for the cytotoxicity studies against the MCF-7 cells.

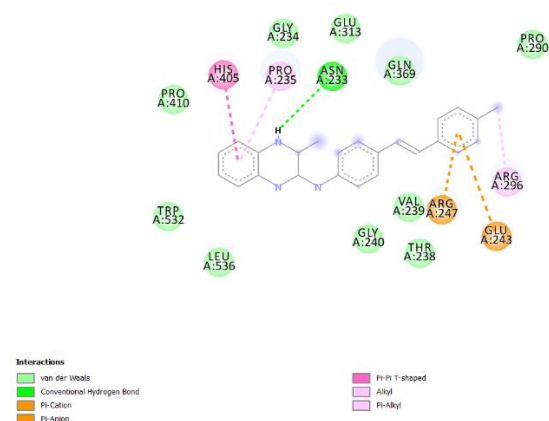


**Figure 4.** 2D docking interaction of compound M2 against AChE

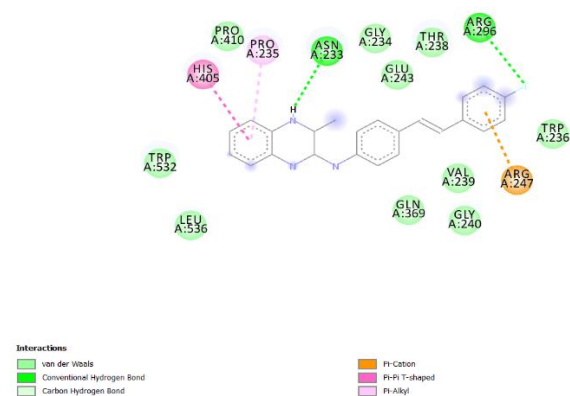


**Figure 5.** 2D docking interaction of compound M3 against AChE

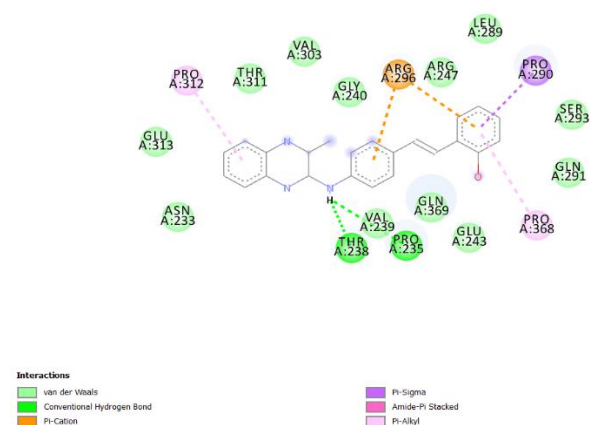


**Figure 6.** 2D docking interaction of compound M4 against AChE

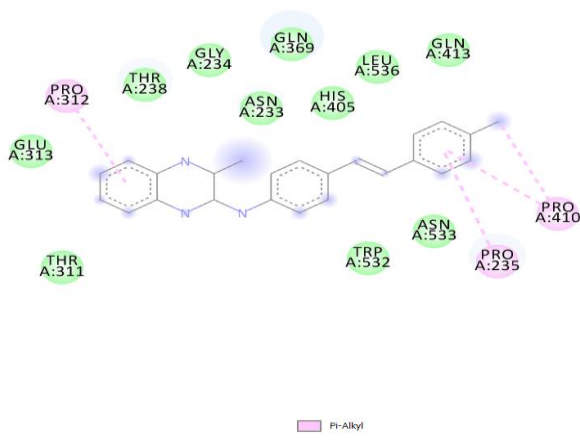


Figure 7. 2D docking interaction of compound M7 against AChE

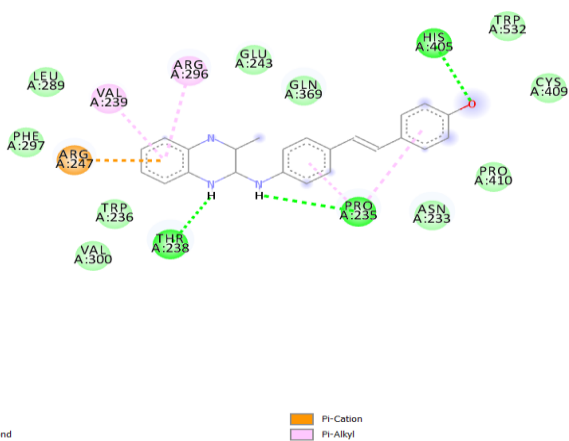


Figure 8. 2D docking interaction of compound M8 against AChE

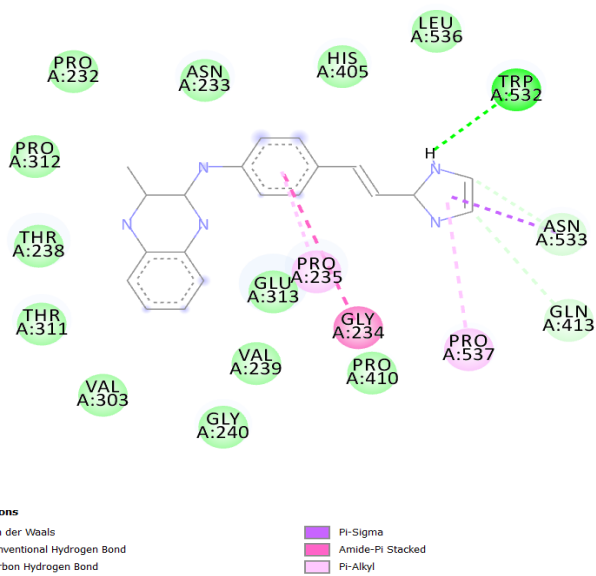
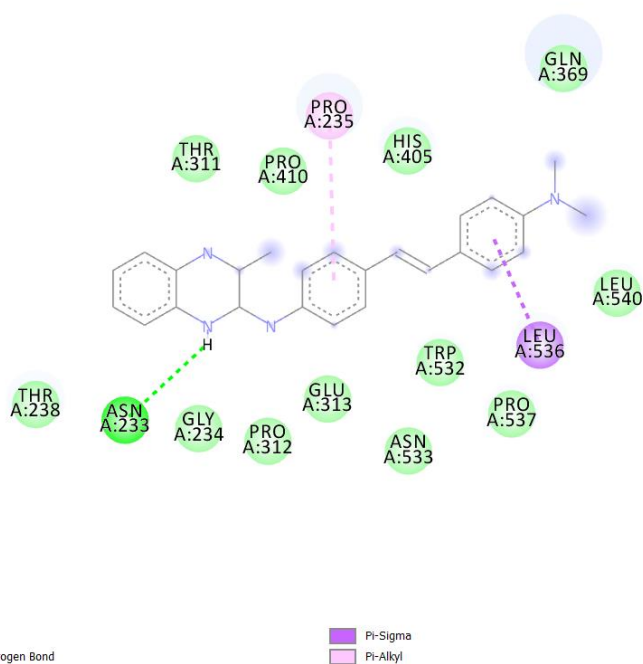


Figure 9. 2D docking interaction of compound M13 against AChE



**Figure 10. 2D docking interaction of compound M14 against AChE**

**Table 3. Binding energy of studied compounds.**

Ligand	Binding Affinity
M1	-7.1
M2	-8.7
M3	-8.1
M4	-8.6
M5	-8.4
M6	-8
M7	-7.9
M8	-7.1
M9	-7.9
M10	-7.4
M11	-7.2
M12	-7.5
M13	-7.9
M14	-7.8
M15	-8.6
Donepezil	-10.28

## 2.10 Chemistry

The final derivatives of quinoxaline hybrid chalcone derivatives were achieved by four step process. In first step, Oxalic acid was dissolved in water, and concentrated hydrochloric acid then add *O*-phenyldiamine. The reaction was refluxed for 20 min. Then it was cooled by addition of ice. The solid was filtered, washed with water, recrystallized from ethanol until 1,4-Dihydro-quinoxaline-2,3-dione was obtained. Further this compound reacts with POCl<sub>3</sub> and pyridine under reflux for 5 hrs. The mixture was allowed to cool, and then poured into crushed ice. The precipitate was filtered and washed with water. 2,3-Dichloro-quinoxaline was recrystallized from ethanol. The third step derivatives were obtained from the chalcone formation reaction between 2,3-dichloroquinoxaline and *p*-methyl aniline in *n*-butanol. It was subjected to irradiation in microwave at 130°C for 30 min. Reaction mixture was allowed to cool at room temperature. The crude product was recrystallization using ethanol. Finally the product obtained from step 3 was added to substituted benzaldehyde in ethanol solvent. The mixture was stirred in ice bath using magnetic stirrer. Then add 10ml of 2N sodium hydroxide and stir for 30min. It is kept undisturbed overnight. The product is neutralized with hydrochloric acid in cold condition. The precipitate obtained is filtered, washed and recrystallized from

ethanol. The completion of the reaction and purity of synthesized compounds were analyzed by TLC using ethylacetate and n-hexane as mobile phase and the synthesized derivatives was subjected to melting point determination. The structure of synthesized compounds was elucidated by various spectral analyses. From the spectral analysis, it evident that all the compounds showed a corresponding signals in all the spectral data. The spectral data for all the compounds are given below:

### 2.10.1 Spectral Data of synthesized compounds

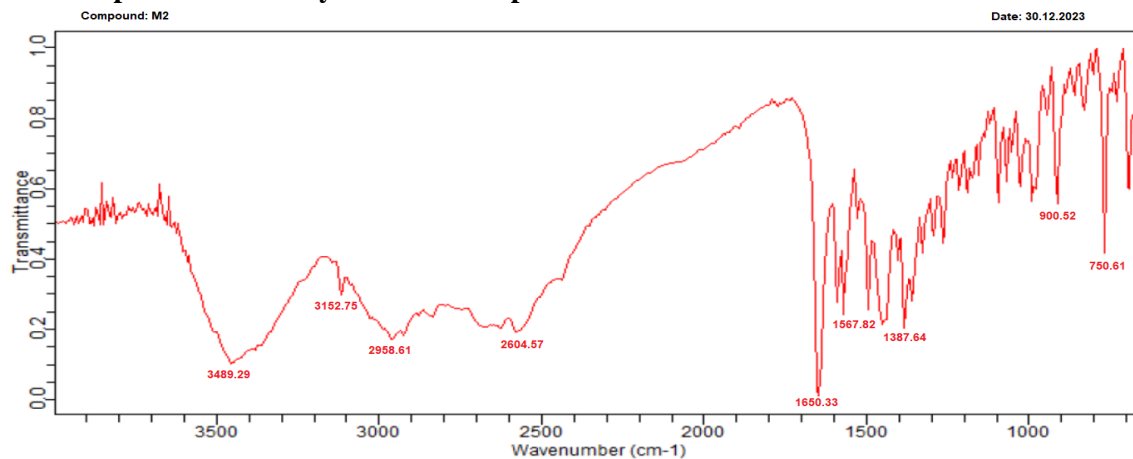


Figure 11: IR Spectra for compound M2

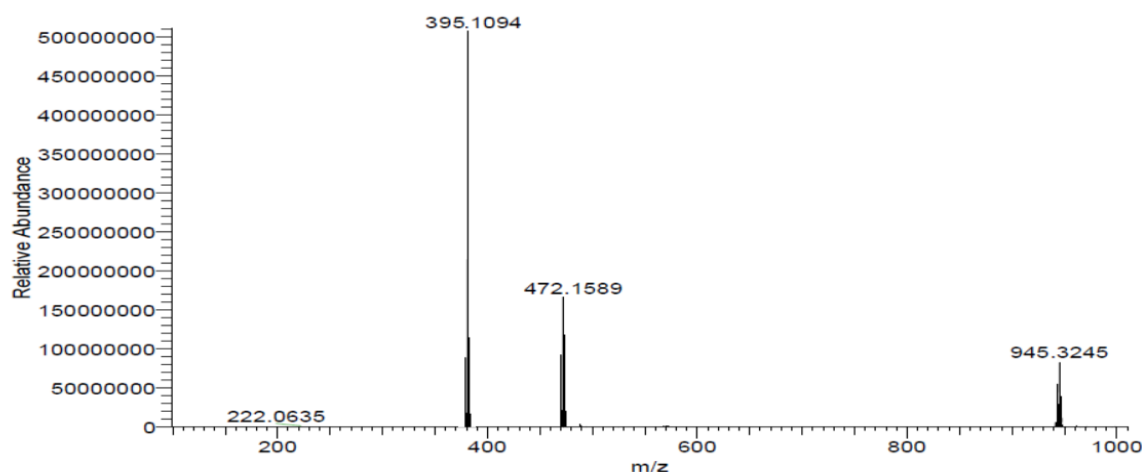


Figure 12: Mass Spectra for compound M2

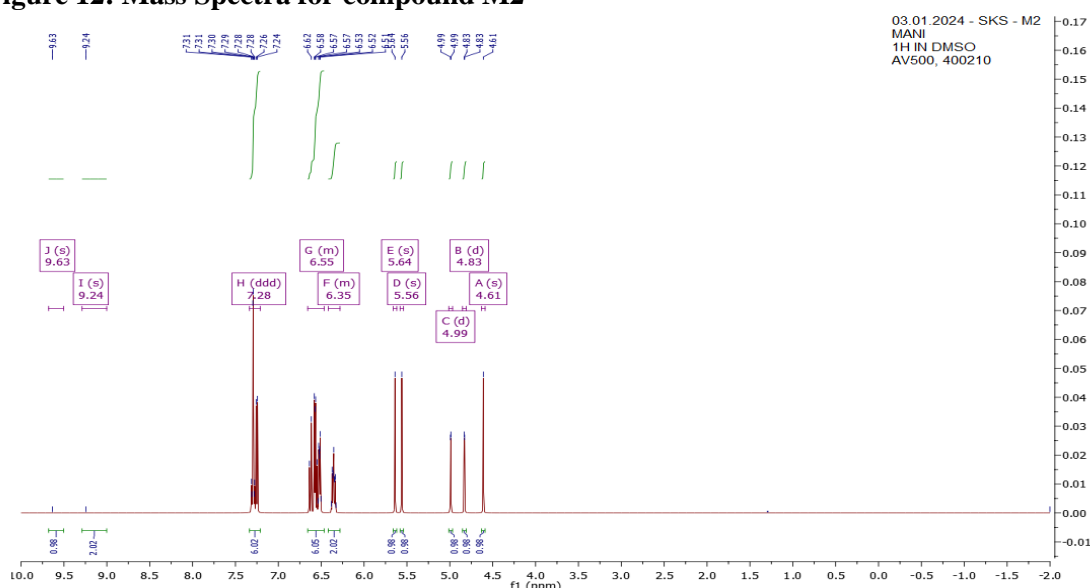


Figure 13:  $^1\text{H}$  NMR Spectra for compound M2

Available online at: <https://jazindia.com>

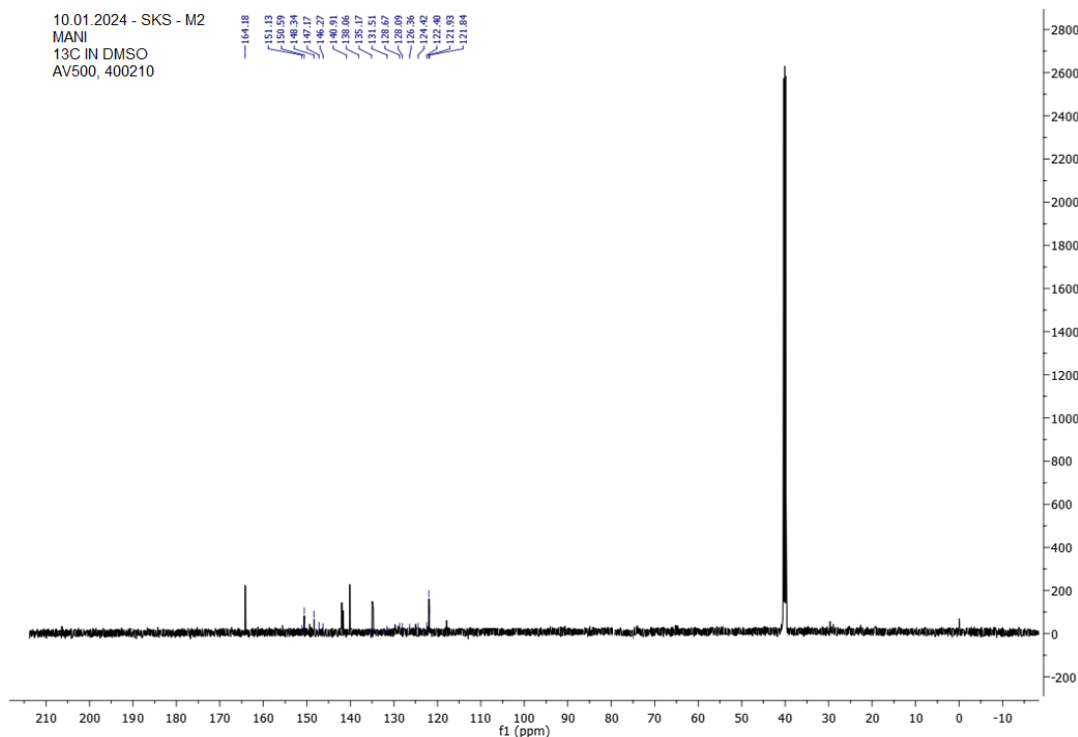


Figure 14: <sup>13</sup>C NMR Spectra for compound M2

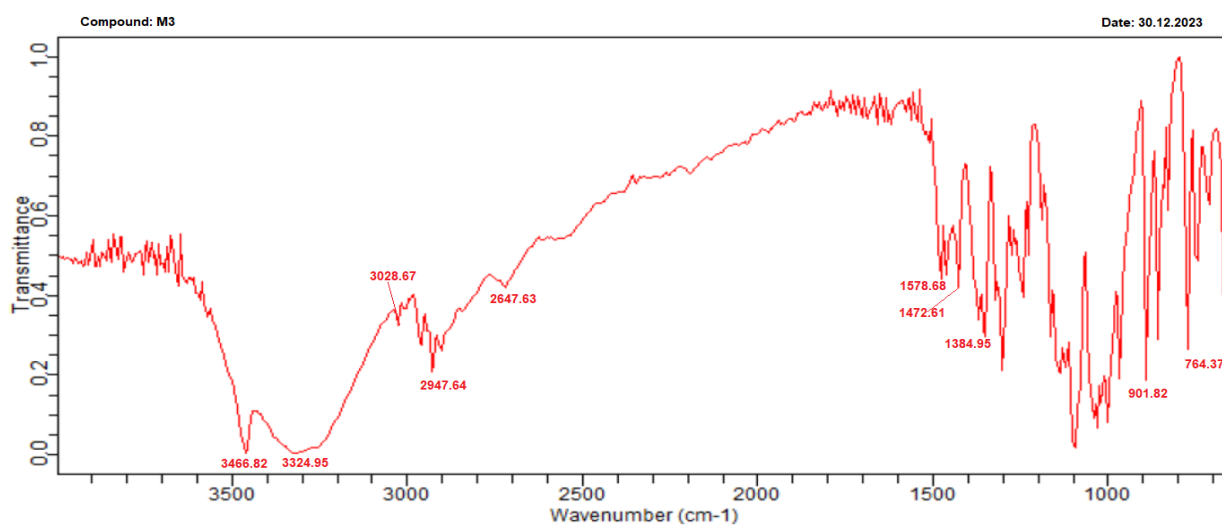


Figure 15: IR Spectra for compound M3

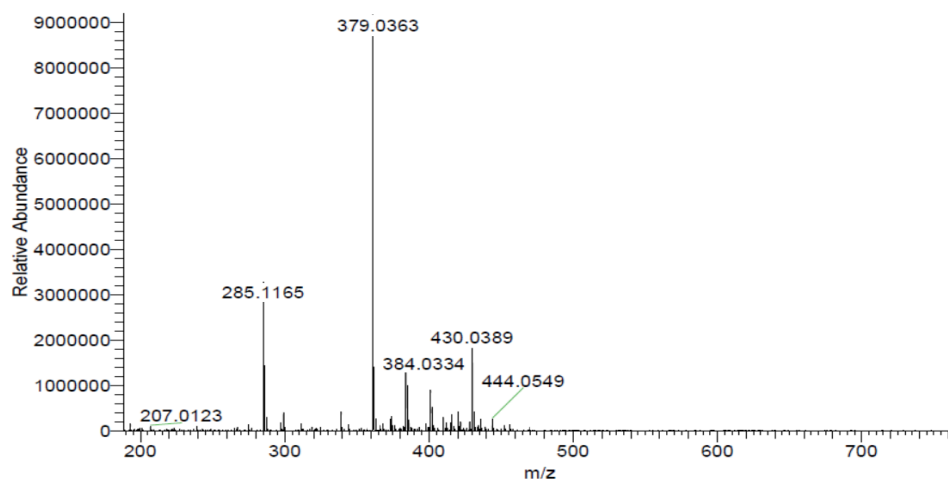


Figure 16: Mass Spectra for compound M3

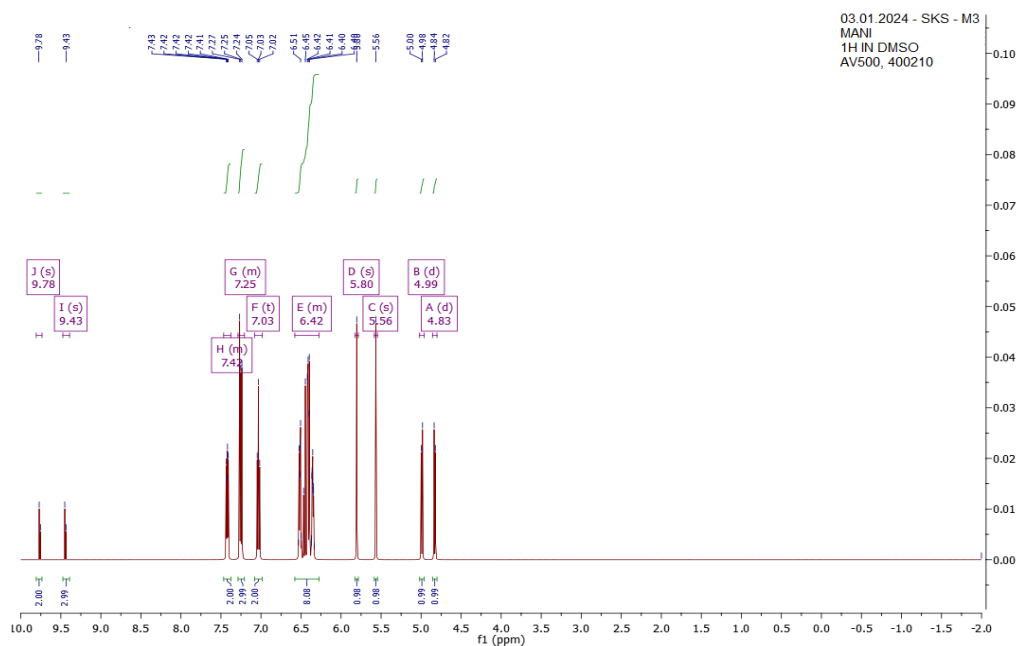


Figure 17: <sup>1</sup>H NMR Spectra for compound M3

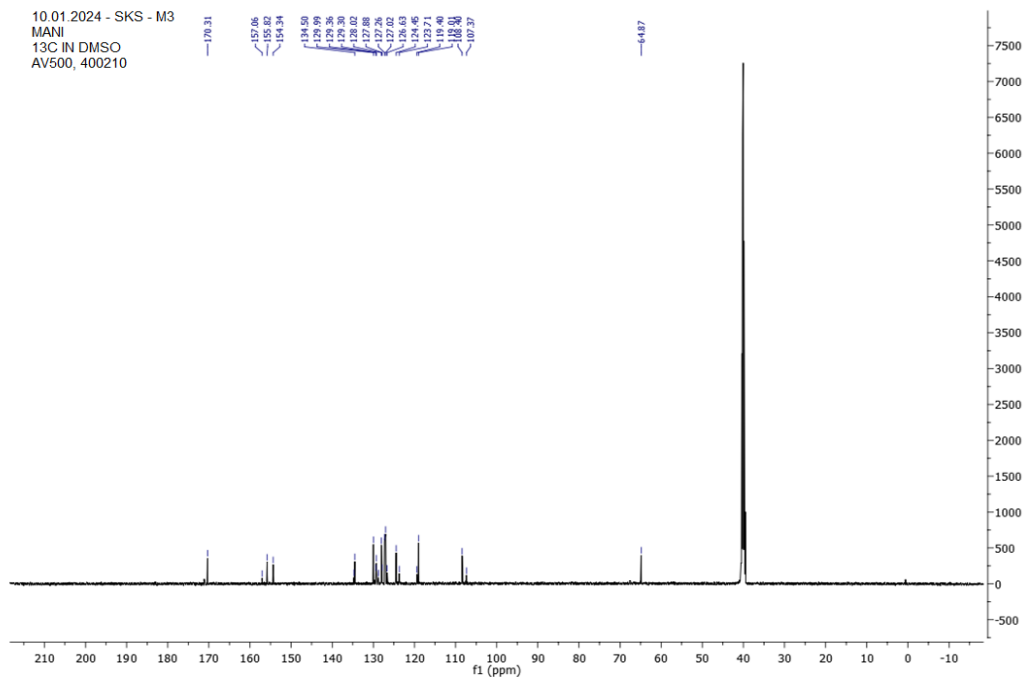


Figure 18: <sup>13</sup>C NMR Spectra for compound M3

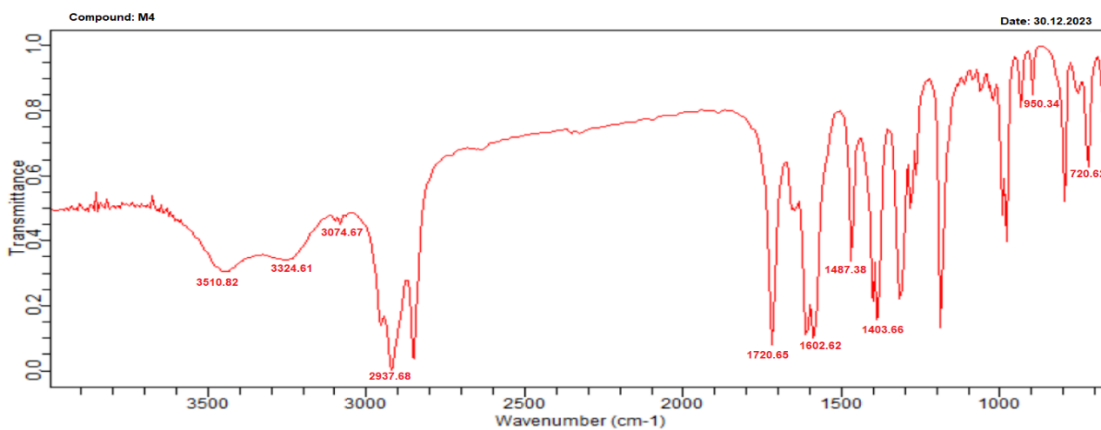


Figure :19 IR Spectra for compound M4

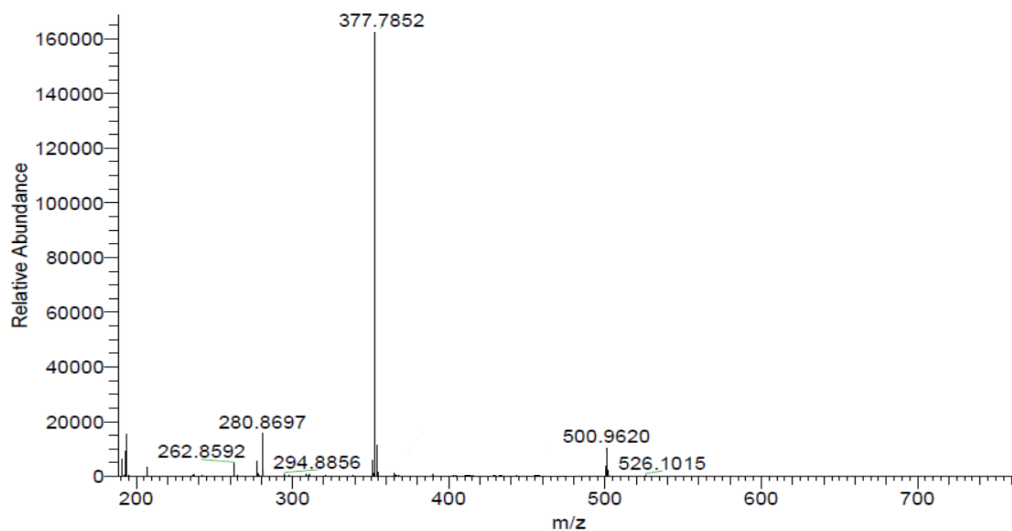


Figure :20 Mass Spectra for compound M4

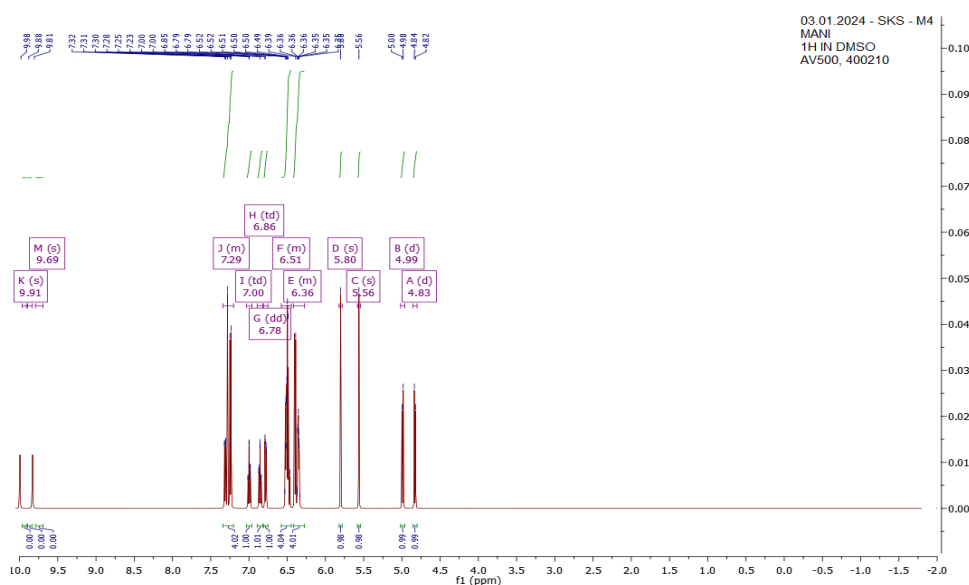


Figure : 21 <sup>1</sup>H Spectra for compound M4

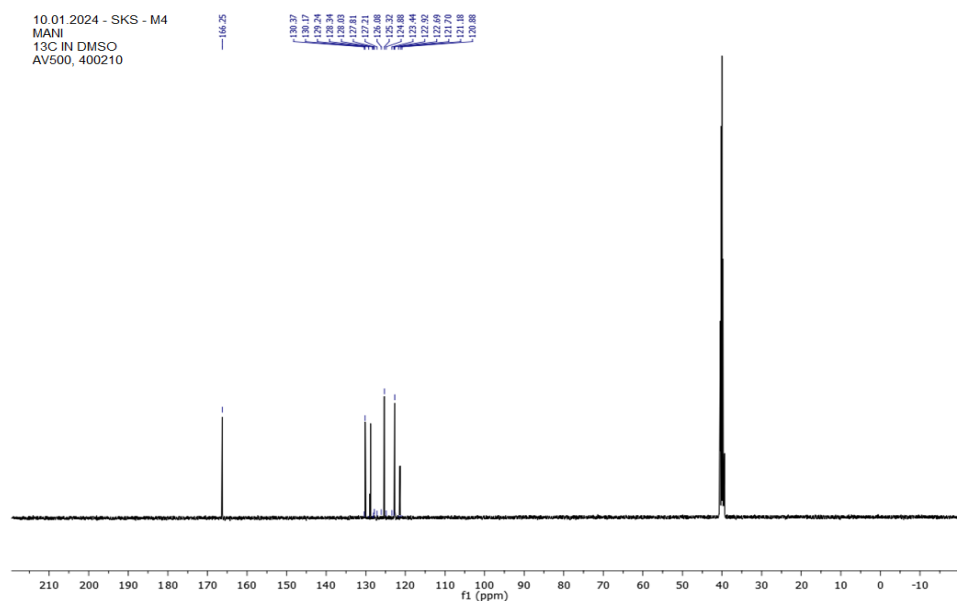


Figure: 22 <sup>13</sup>C NMR Spectra for compound M4

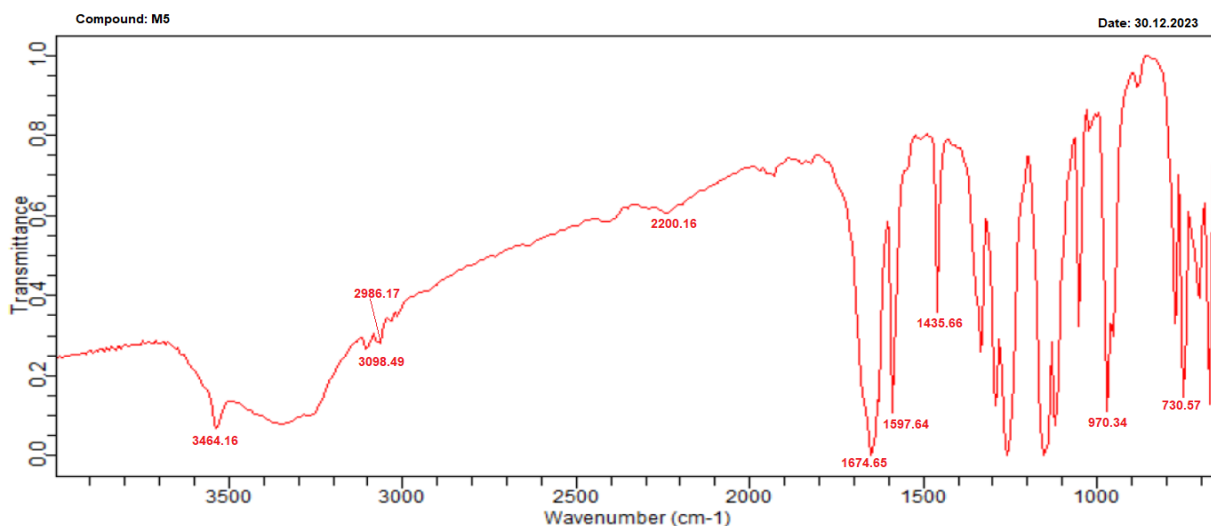


Figure: 23 IR Spectra for compound M5

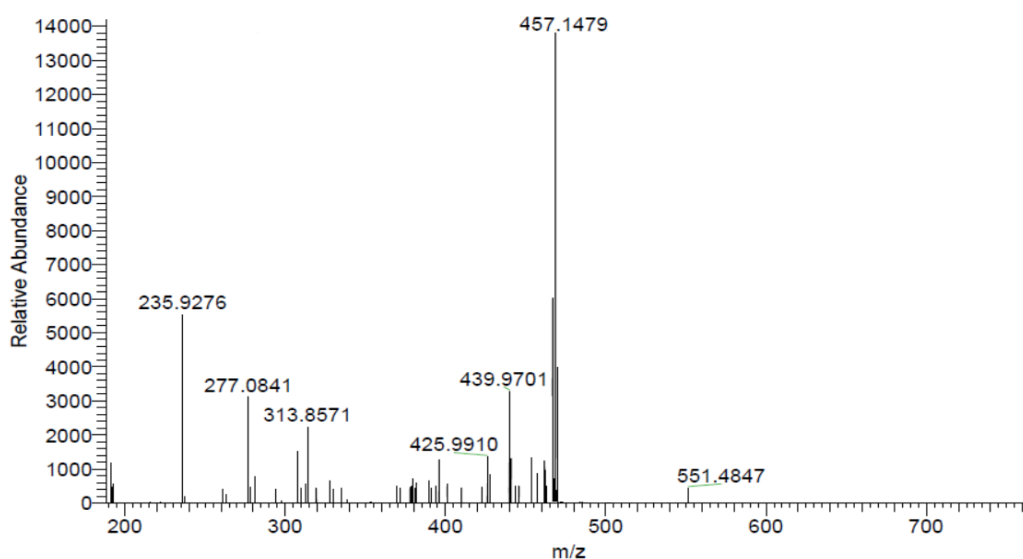
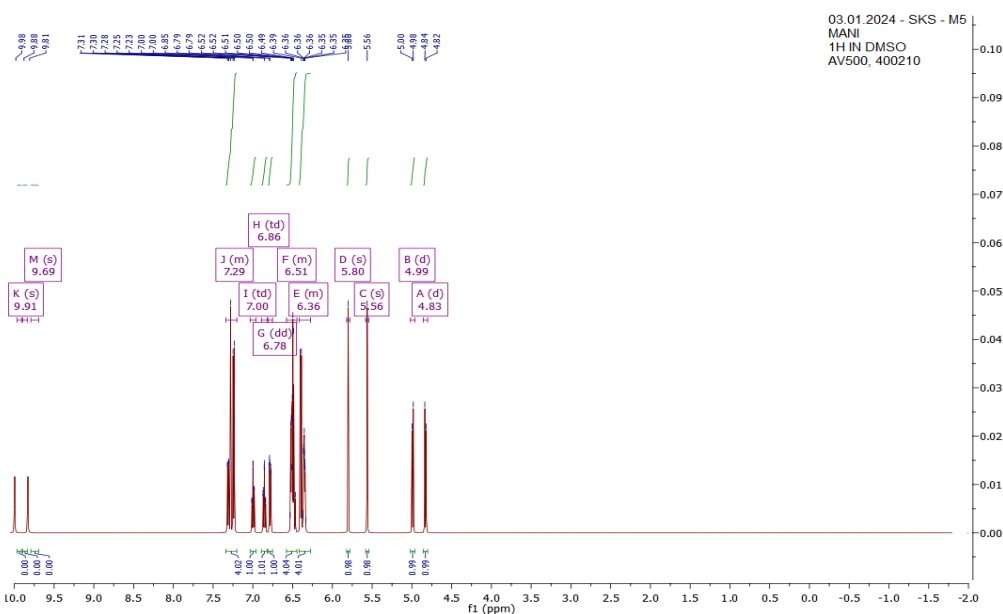


Figure : 24 Mass Spectra for compound M5

Figure : 25 <sup>1</sup>H NMR Spectra for compound M5Available online at: <https://jazindia.com>

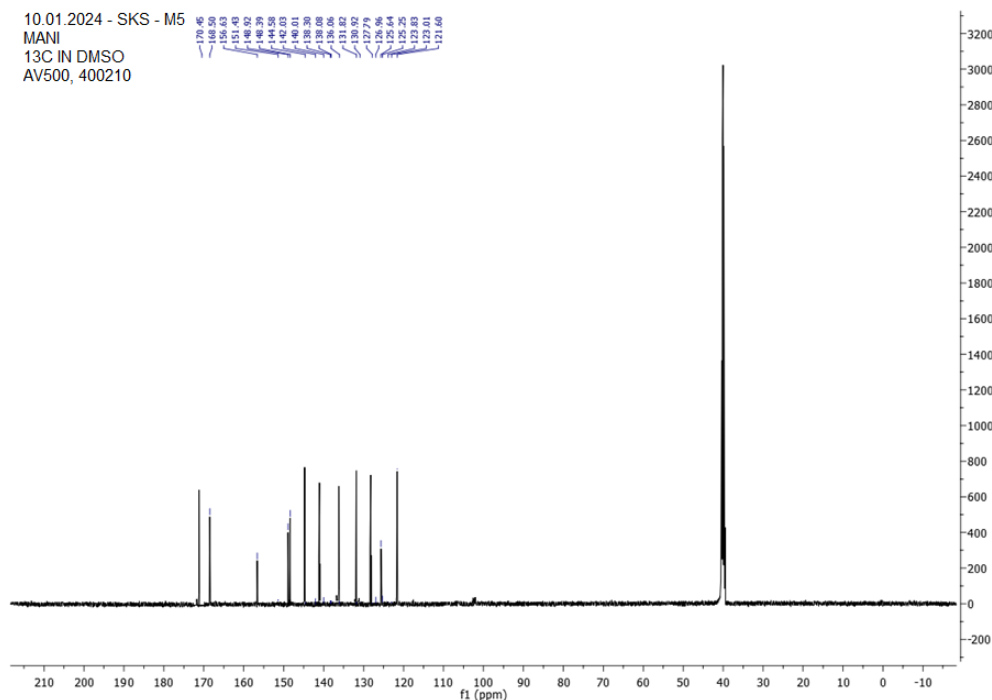


Figure : 26 <sup>13</sup>C NMR Spectra for compound M5

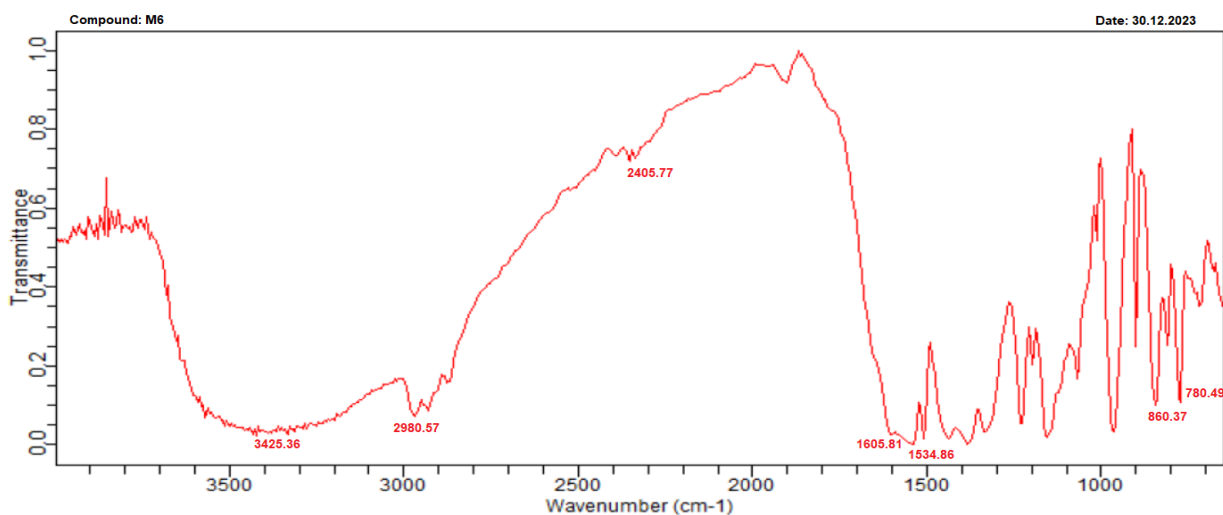


Figure : 27 IR Spectra for compound M6

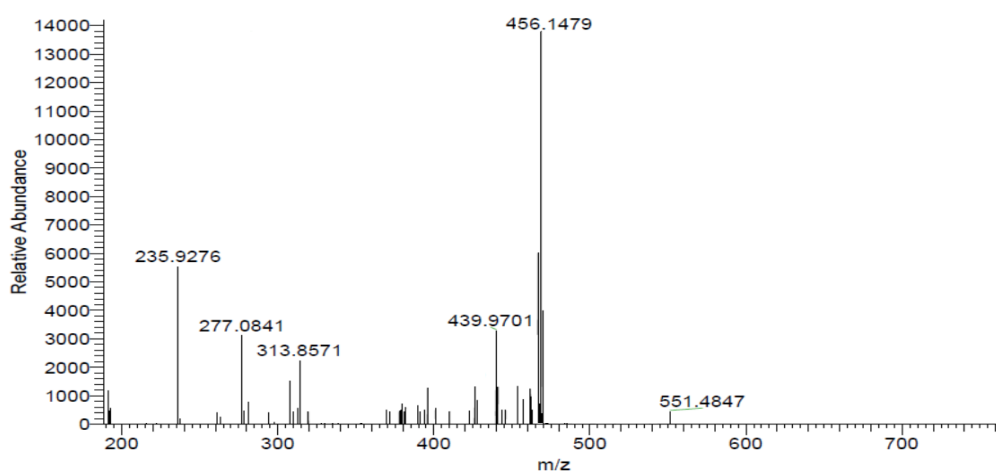


Figure: 28 Mass Spectra for compound M6

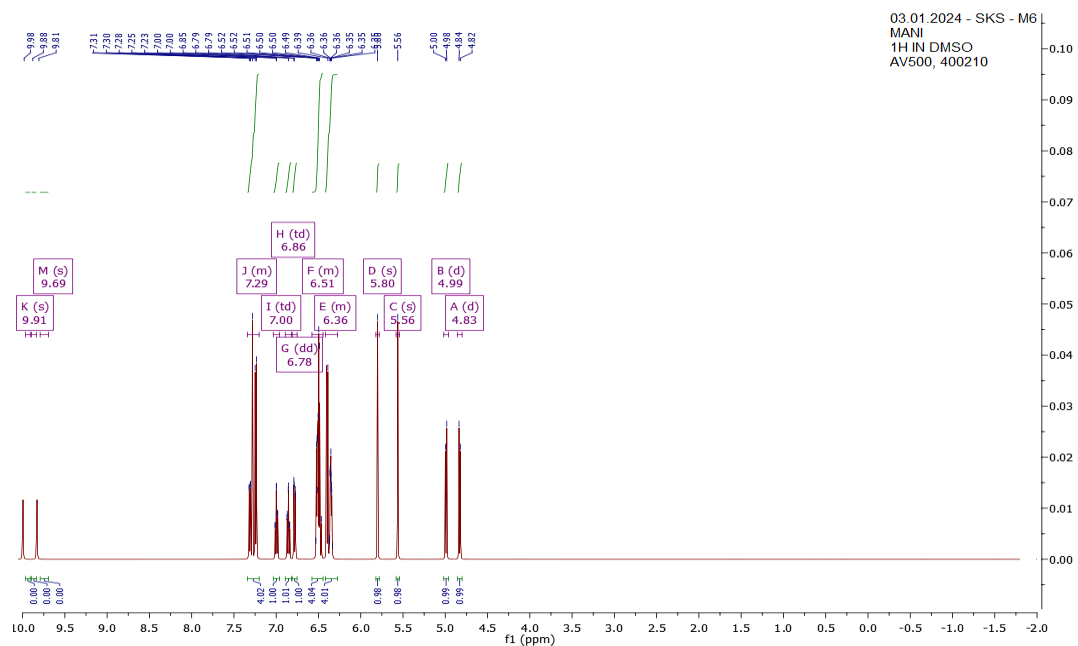


Figure: 29 <sup>1</sup>H NMR Spectra for compound M6

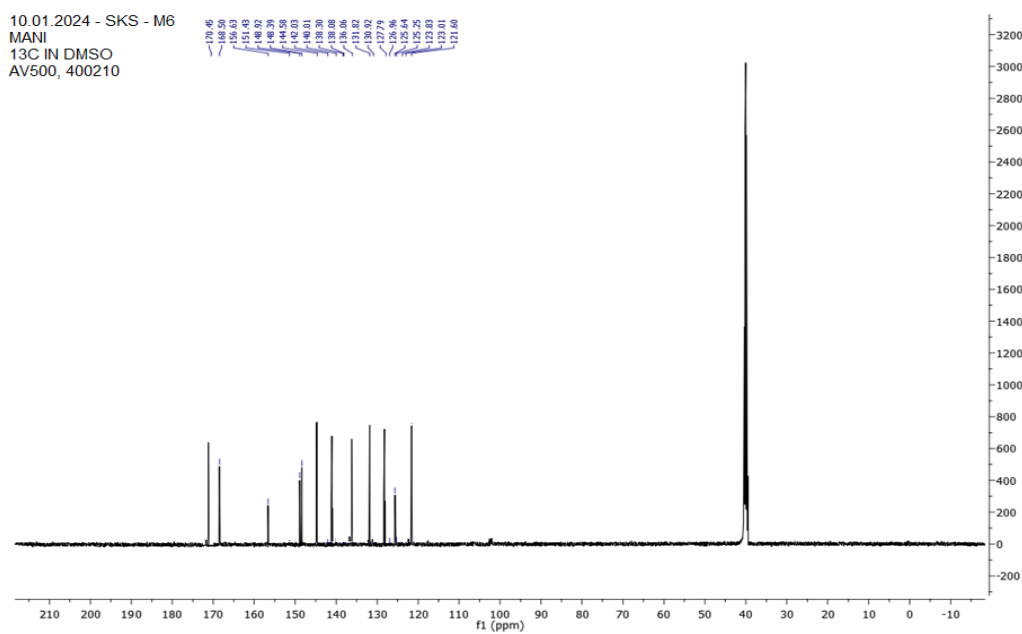


Figure: 30 <sup>13</sup>C NMR Spectra for compound M6

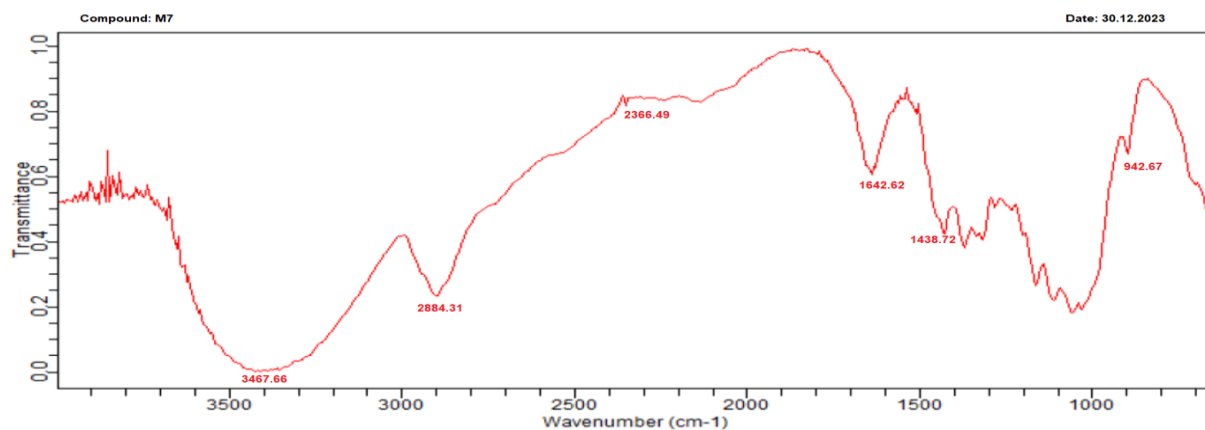


Figure : 31 IR Spectra for compound M7

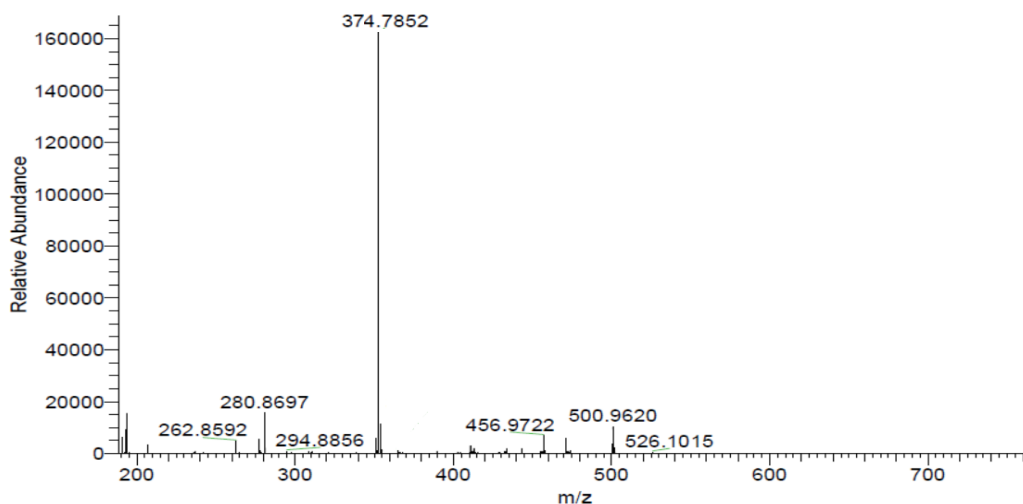


Figure : 32 Mass Spectra for compound M7

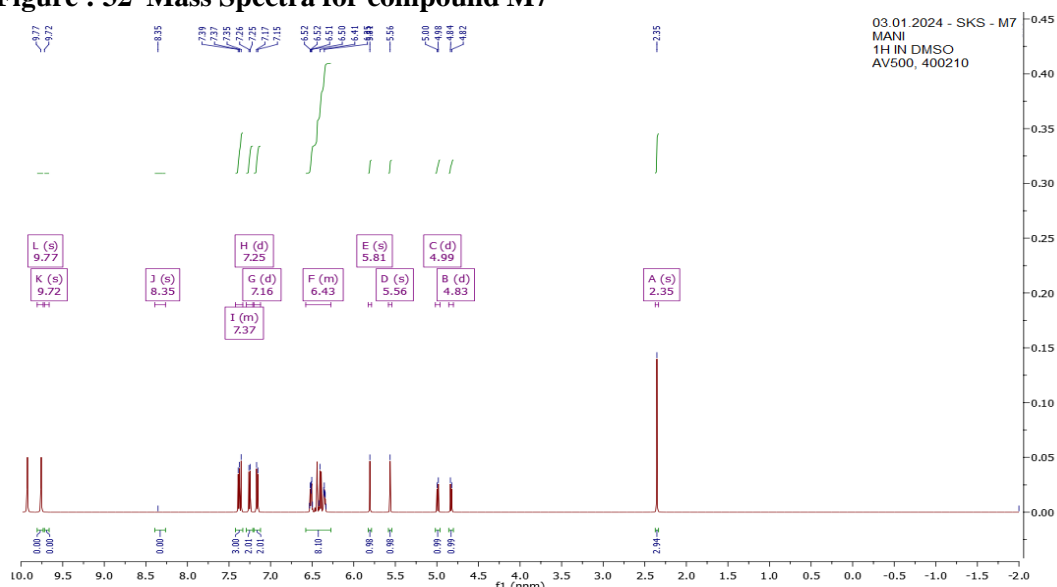


Figure : 33 <sup>1</sup>H NMR Spectra for compound M7

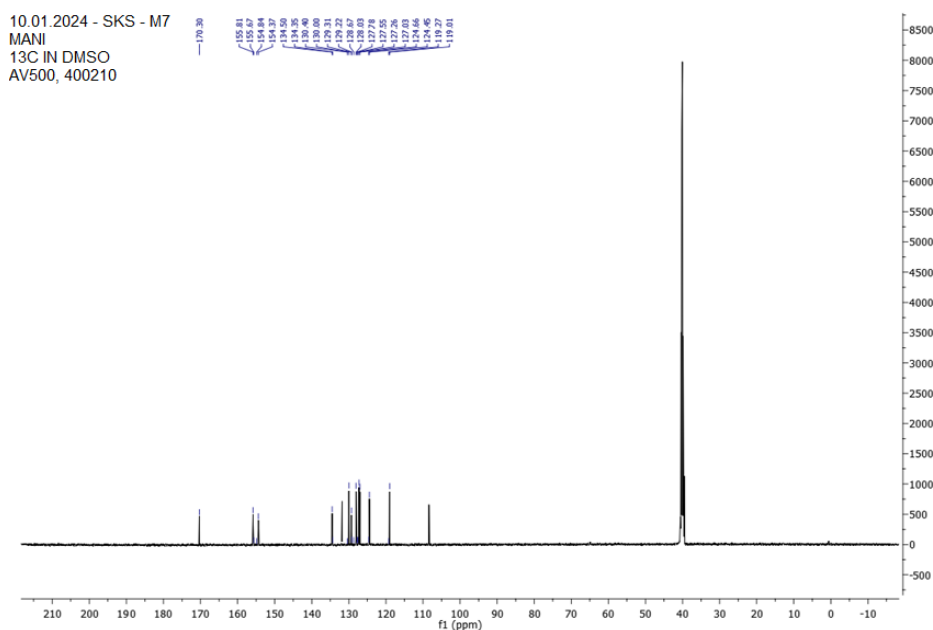


Figure: 34 <sup>13</sup>C NMR Spectra for compound M7

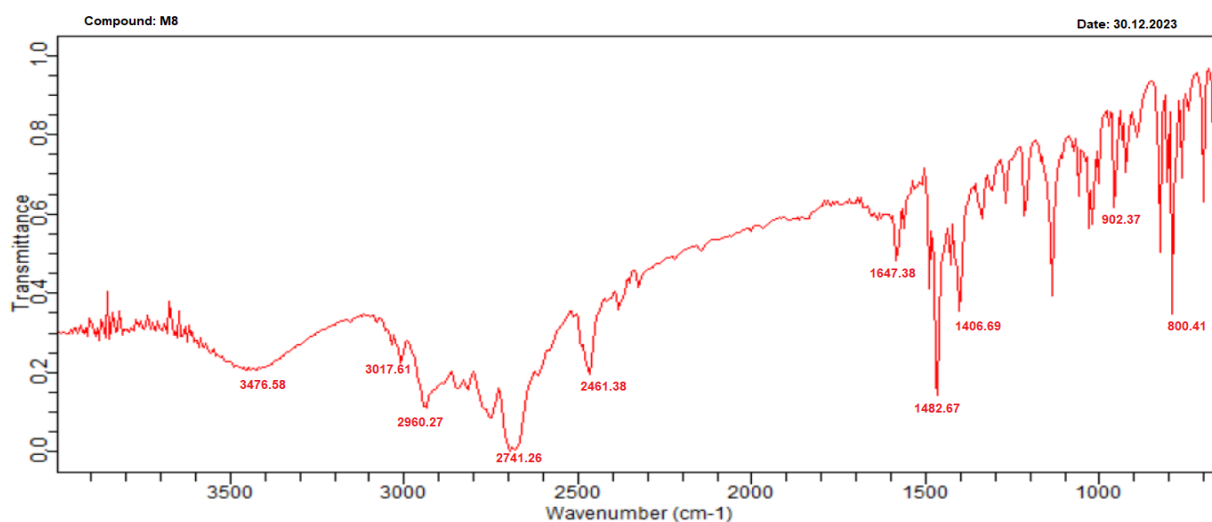


Figure : 35 IR Spectra for compound M8

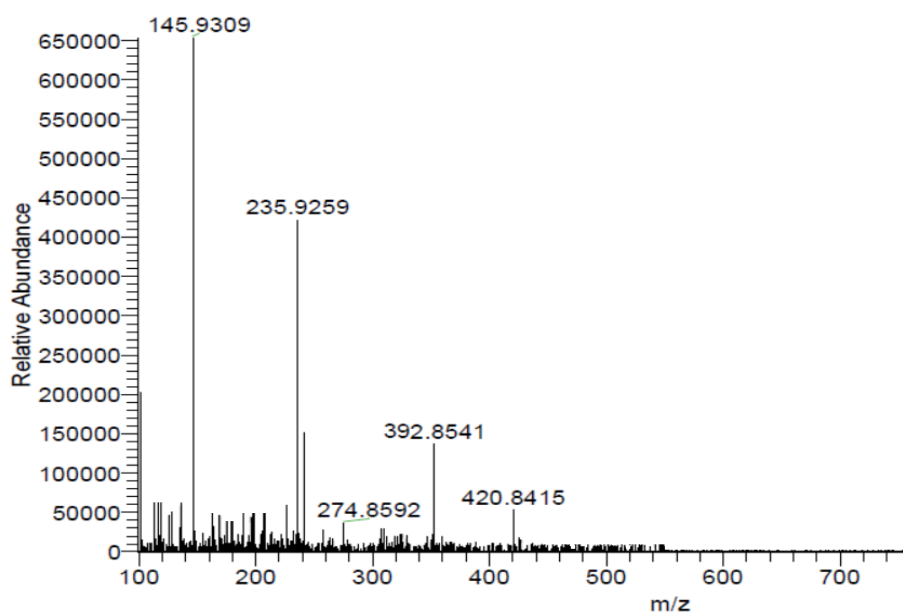
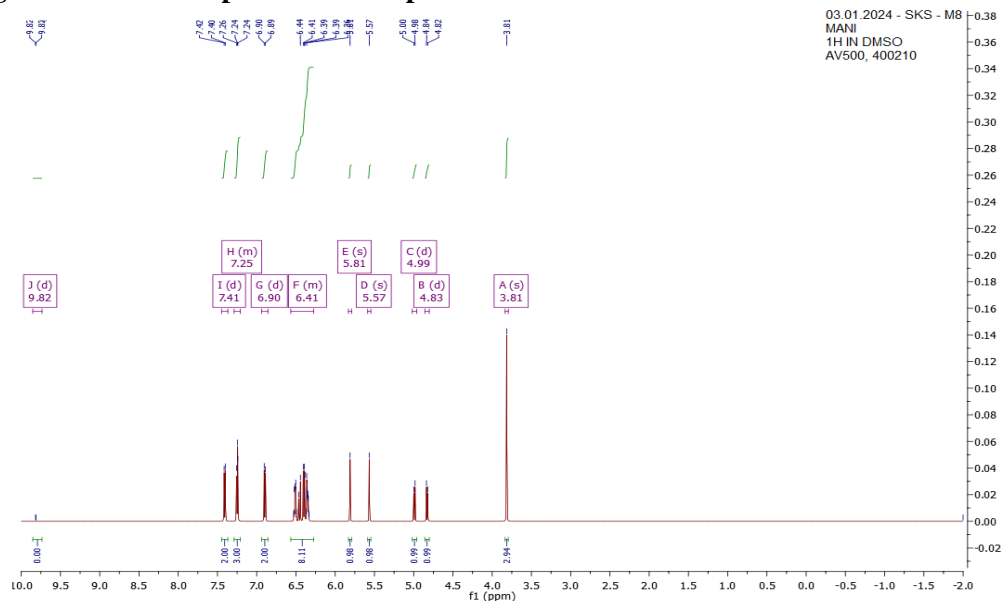


Figure : 36 Mass Spectra for compound M8

Figure : 37  $^1\text{H}$  NMR Spectra for compound M8

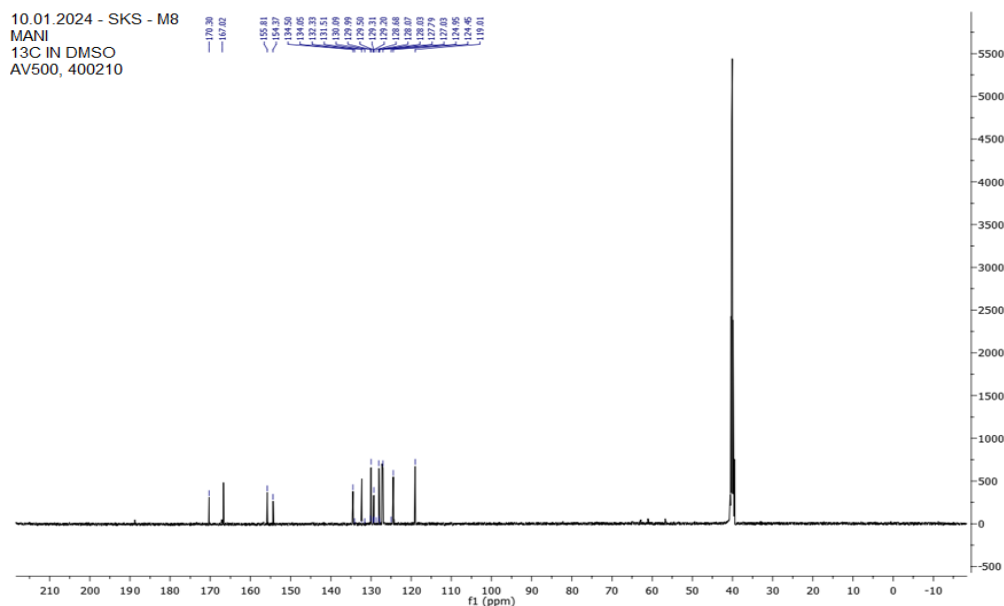


Figure : 38 <sup>13</sup>C NMR Spectra for compound M8

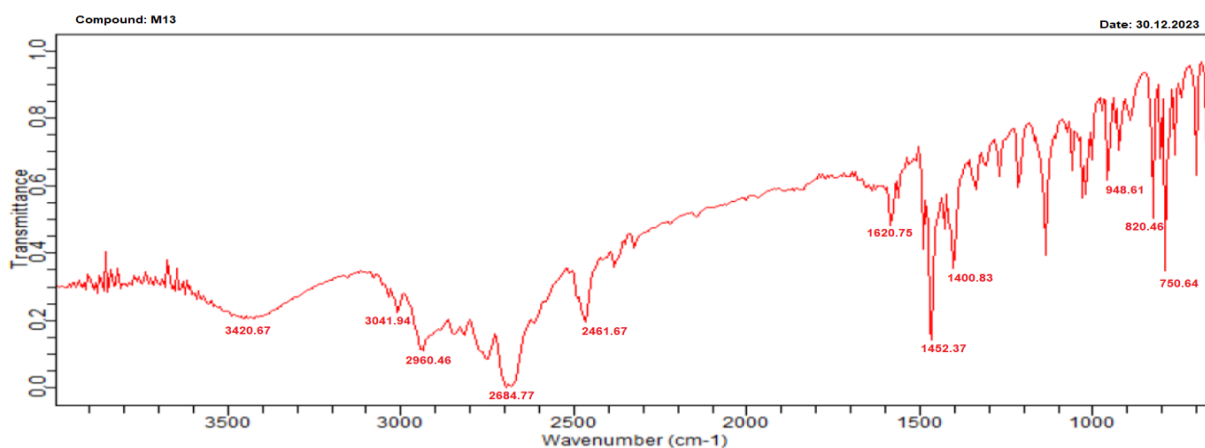


Figure :39 IR Spectra for compound M13

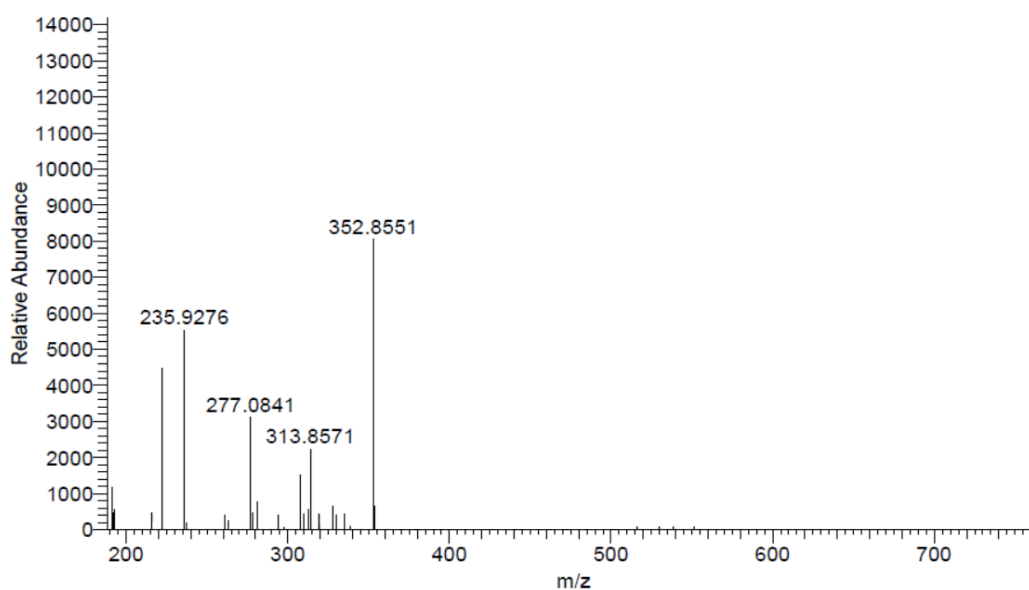


Figure : 40 Mass Spectra for compound M13

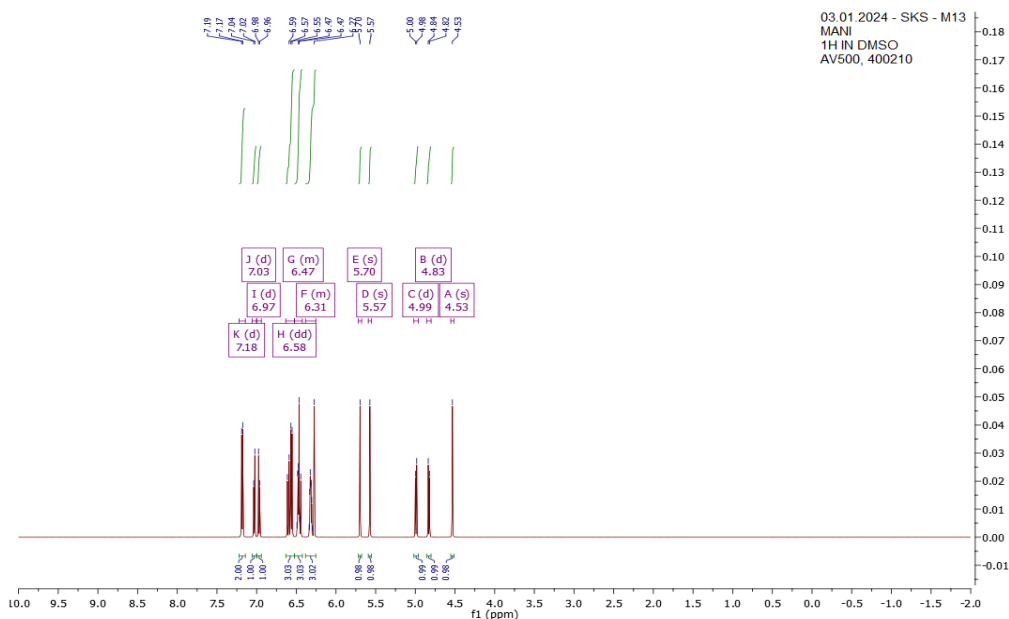


Figure :41 <sup>1</sup>H NMR Spectra for compound M13

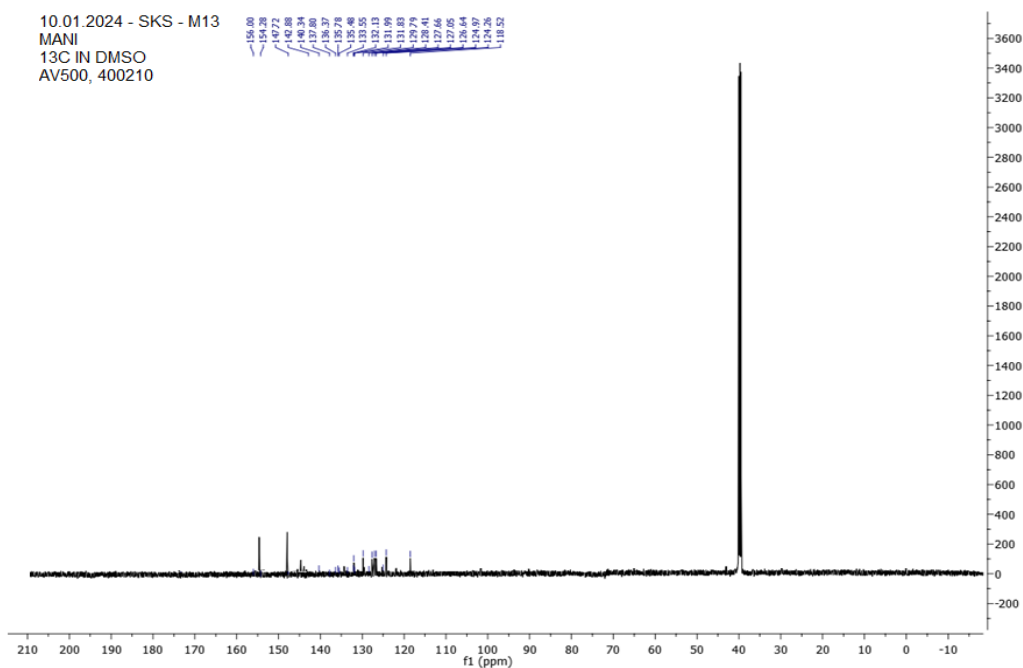


Figure: 42 <sup>13</sup>C NMR Spectra for compound M13

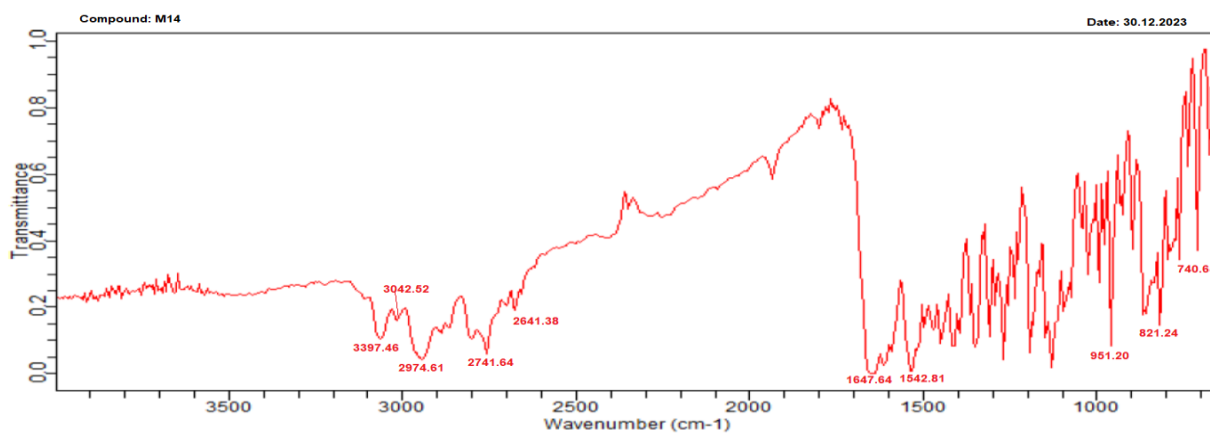


Figure: 43 IR Spectra for compound M14

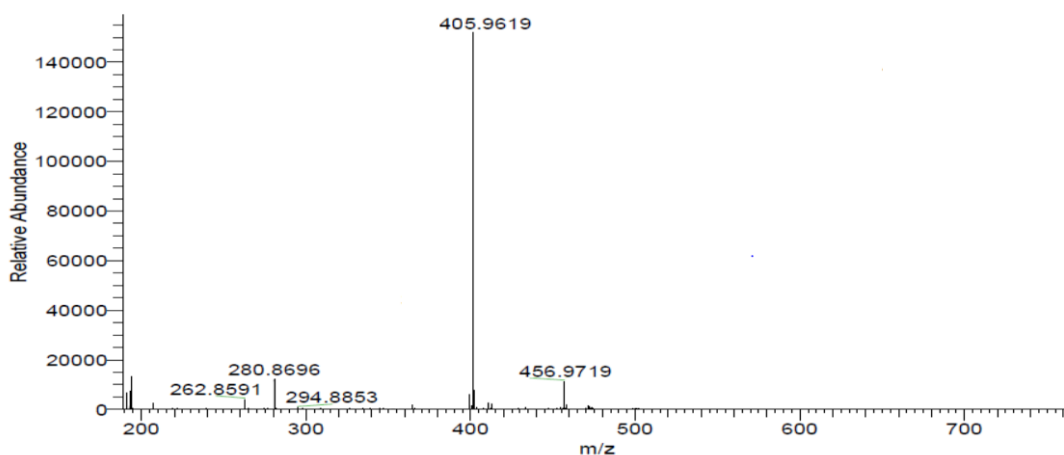


Figure : 44 Mass Spectra for compound M14

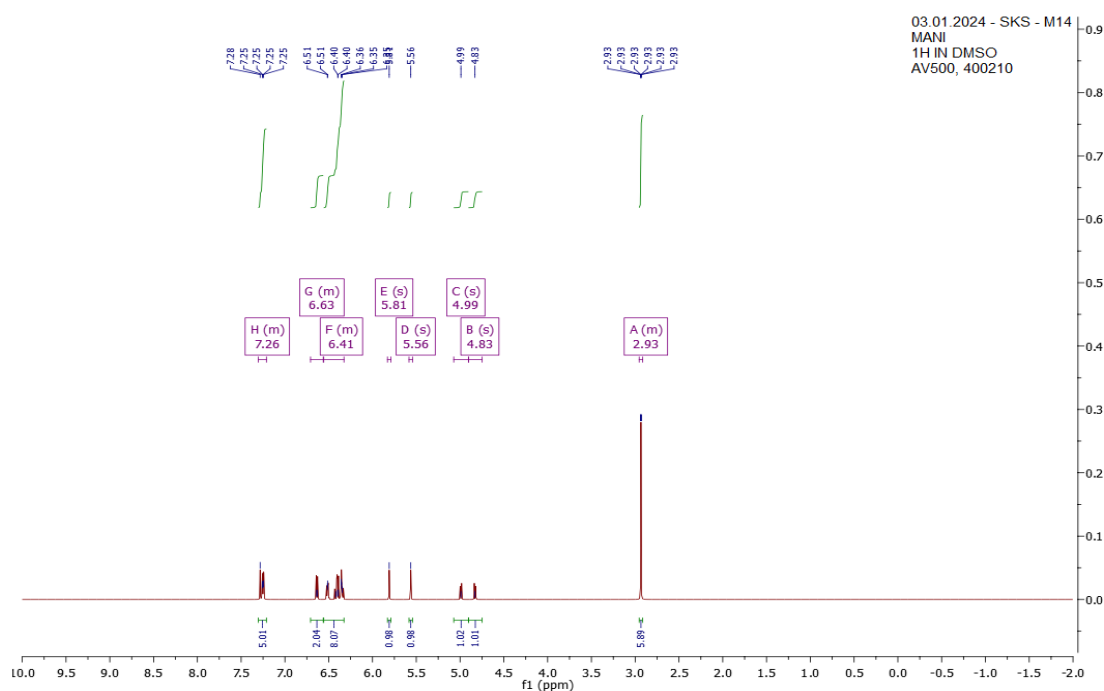


Figure: 45 <sup>1</sup>H NMR Spectra for compound M14

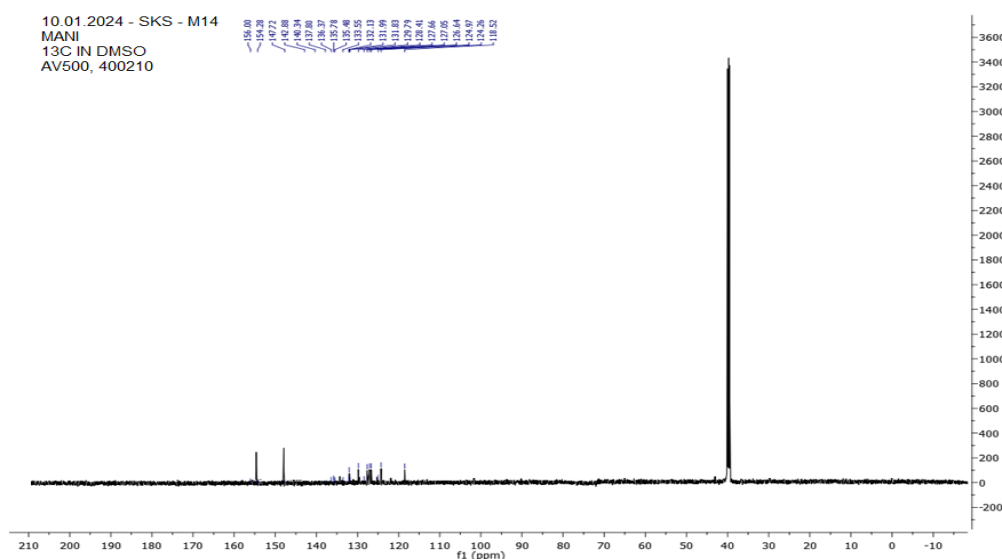


Figure : 46 <sup>13</sup>C NMR Spectra for compound M14

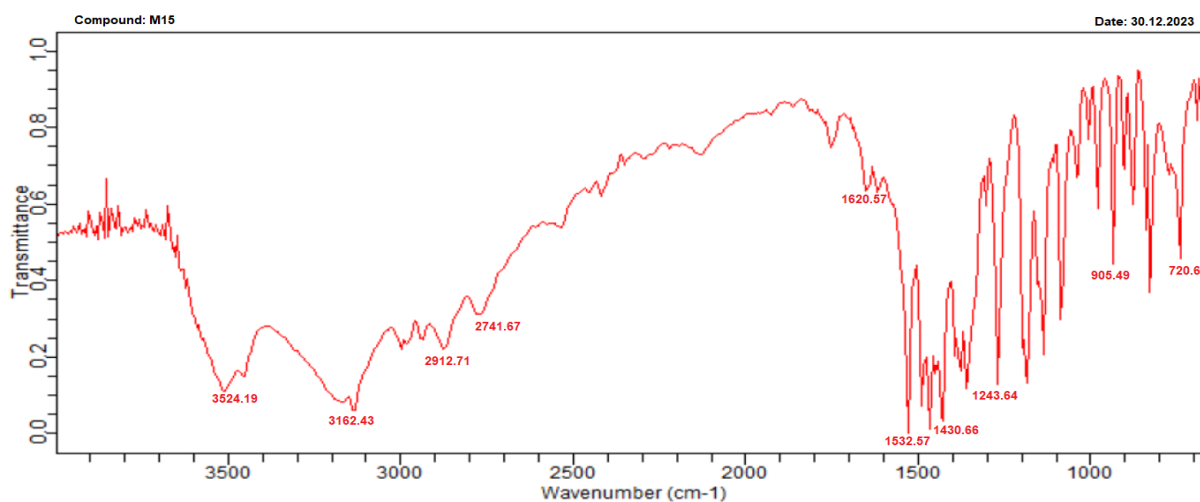


Figure : 47 IR Spectra for compound M15

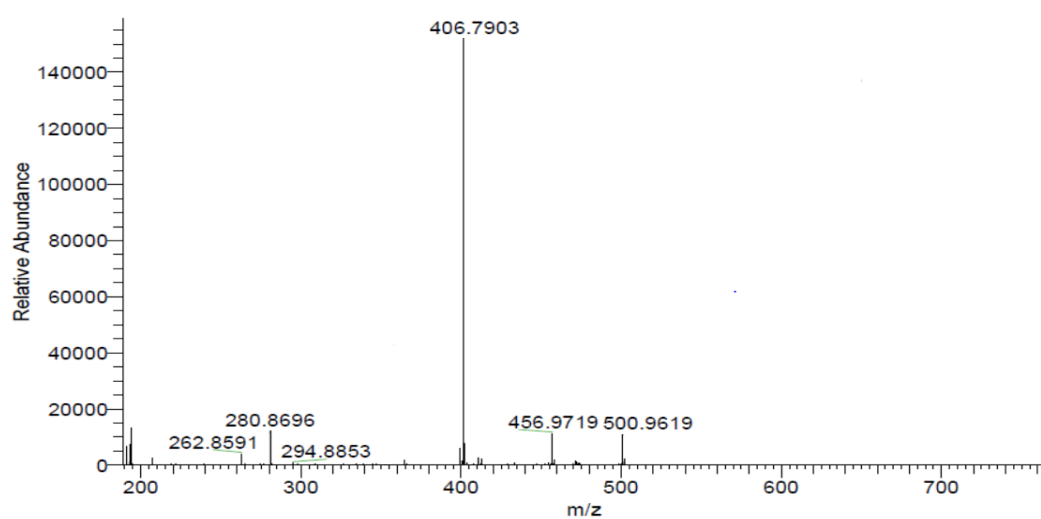
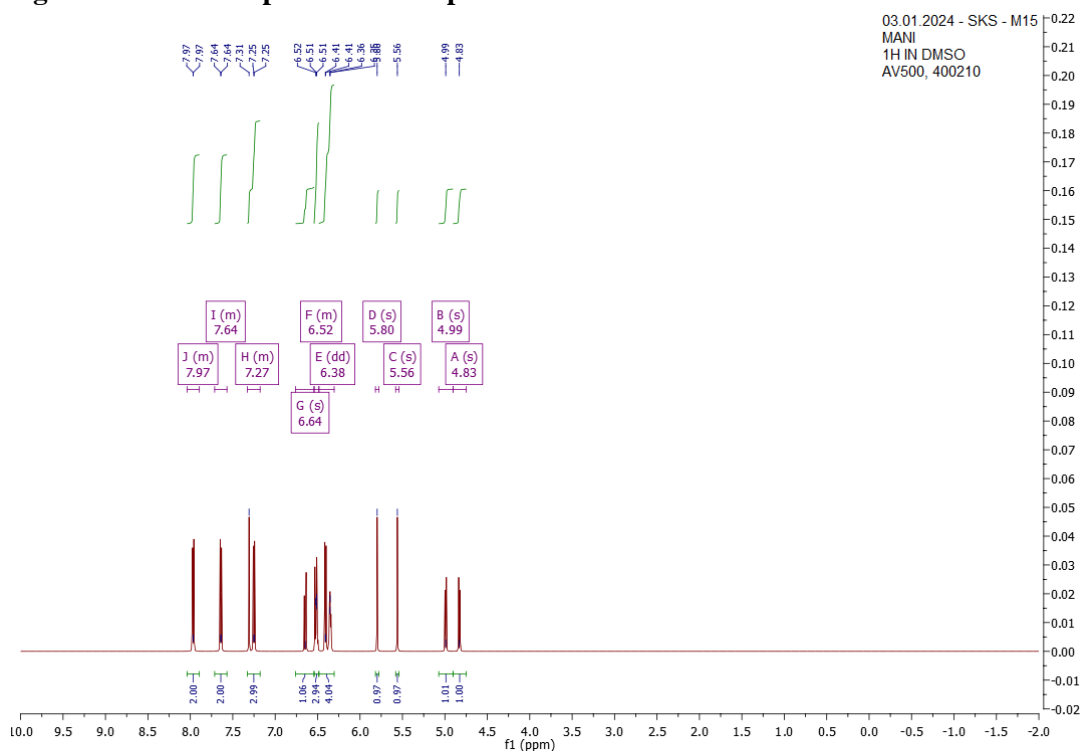


Figure : 48 Mass Spectra for compound M15

Figure : 49 <sup>1</sup>H NMR Spectra for compound M15

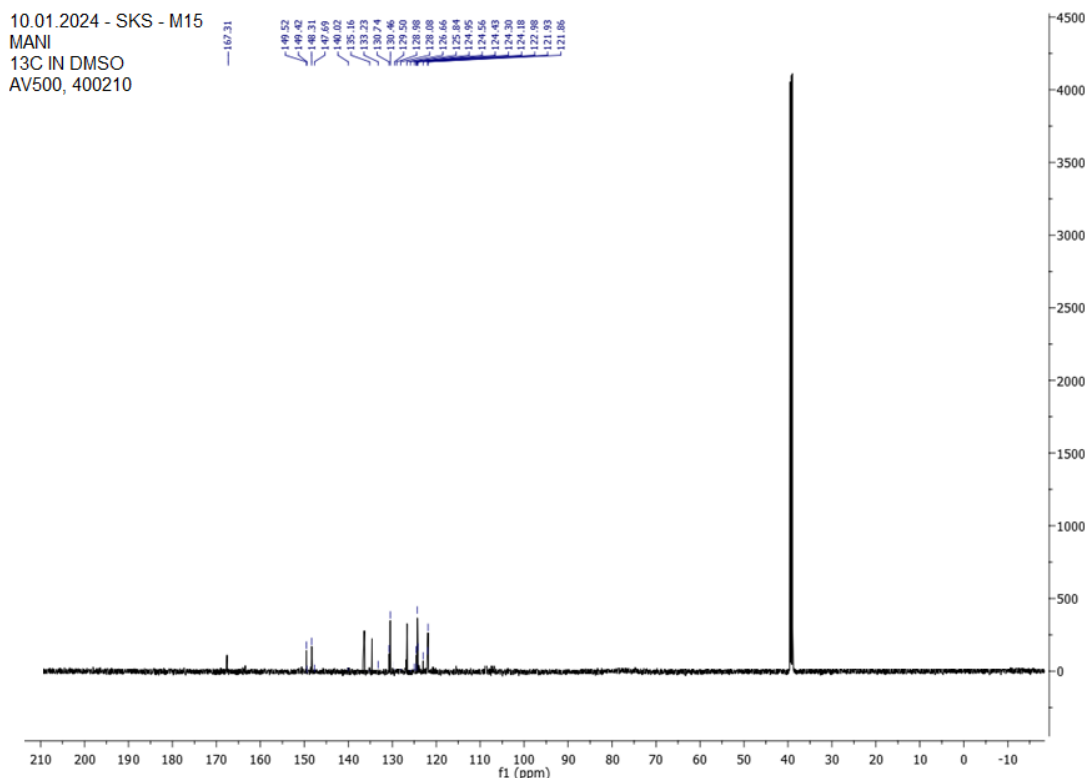


Figure : 50  $^{13}\text{C}$  NMR Spectra for compound M15

#### 5.4.2. Characterization of synthesized compounds

##### 5.4.2.1. (Z)-3-chloro-N-(4-(4-chlorostyryl)phenyl)-1,2,3,4-tetrahydroquinoxalin-2-amine (M2)

$\text{C}_{22}\text{H}_{19}\text{Cl}_2\text{N}_3$ ; Red colour solid; MP: 102 – 105 $^{\circ}\text{C}$ ; Rf: 0.47; IR (KBr)  $\text{cm}^{-1}$ : 3489 (NH str, Amine) 3152 (CH str alkene); 2958 (CH str alkane); 2604 (CH str aromatic); 1387 (CN bending); 900 (Aromatic ring); 750 (C-Cl str);  $^1\text{H}$  NMR (500 MHz, DMSO)  $\delta$  9.63 (s, 2H), 9.24 (s, 1H), 7.28 (ddd,  $J = 18.2, 12.3, 4.5$  Hz, 1H), 6.66 – 6.47 (m, 2H), 6.42 – 6.28 (m, 1H), 5.64 (s, 1H), 5.56 (s, 1H), 4.99 (d,  $J = 2.0$  Hz, 1H), 4.83 (d,  $J = 2.0$  Hz, 1H), 4.61 (s, 1H);  $^{13}\text{C}$  NMR (126 MHz, DMSO):  $\delta$  164.18, 151.13, 150.59, 148.34, 147.17, 146.27, 140.91, 138.06, 135.17, 131.51, 128.67, 128.09, 126.36, 124.42, 122.40, 121.93, 121.84; Mass: Actual: 396 m/z; Found: 395 (M-1) m/z.

##### 5.4.2.2. (Z)-3-chloro-N-(4-(4-fluorostyryl)phenyl)-1,2,3,4-tetrahydroquinoxalin-2-amine (M3)

$\text{C}_{22}\text{H}_{19}\text{ClFN}_3$ ; brown solid; MP: 104 – 107 $^{\circ}\text{C}$ ; Rf: 0.51; IR (KBr)  $\text{cm}^{-1}$ : 3466 (NH str, Amine) 3027 (CH str alkene); 2947 (CH str alkane); 2647 (CH str aromatic); 1384 (CN bending); 901 (Aromatic ring); 764 (C-Cl str);  $^1\text{H}$  NMR (500 MHz, DMSO)  $\delta$  9.78 (s, 1H), 9.43 (s, 1H), 7.47 – 7.38 (m, 1H), 7.29 – 7.21 (m, 2H), 7.03 (t,  $J = 7.7$  Hz, 2H), 6.58 – 6.28 (m, 2H), 5.80 (s, 1H), 5.56 (s, 1H), 4.99 (d,  $J = 7.9$  Hz, 1H), 4.83 (d,  $J = 7.9$  Hz, 1H).  $^{13}\text{C}$  NMR (126 MHz, DMSO):  $\delta$  170.31, 157.06, 155.82, 154.34, 134.70, 134.50, 129.99, 129.36, 129.30, 128.79, 128.02, 127.88, 127.26, 127.02, 126.63, 124.45, 123.71, 119.40, 119.01, 108.40, 107.37, 64.87; Mass: Actual: 379 m/z; Found: 379 m/z.

##### 5.4.2.3. (Z)-2-(4-((3-chloro-1,2,3,4-tetrahydroquinoxalin-2-yl)amino)styryl)phenol (M4)

$\text{C}_{22}\text{H}_{20}\text{ClN}_3\text{O}$ ; brown solid; MP: 111 – 113 $^{\circ}\text{C}$ ; Rf: 0.54; IR (KBr)  $\text{cm}^{-1}$ : 3510 (OH str); 3324 (NH str, Amine) 3074 (CH str alkene); 2937 (CH str alkane); 2604 (CH str aromatic); 1403 (CN bending); 950 (Aromatic ring); 720 (C-Cl str);  $^1\text{H}$  NMR (500 MHz, DMSO)  $\delta$  9.91 (s, 1H), 9.88 (s, 2H), 9.69 (s, 4H), 7.34 – 7.20 (m, 1H), 7.00 (td,  $J = 7.5, 1.4$  Hz, 1H), 6.86 (td,  $J = 7.5, 1.6$  Hz, 2H), 6.78 (dd,  $J = 7.5, 1.5$  Hz, 1H), 6.58 – 6.45 (m, 1H), 6.42 – 6.28 (m, 1H), 5.80 (s, 2H), 5.56 (s, 1H), 4.99 (d,  $J = 7.9$  Hz, 1H), 4.83 (d,  $J = 7.9$  Hz, 1H).  $^{13}\text{C}$  NMR (101 MHz, DMSO):  $\delta$  166.25, 130.37, 130.17, 129.24, 128.34, 128.03, 127.81, 127.21, 126.08, 125.32, 124.88, 123.44, 122.92, 122.69, 121.70, 121.18, 120.88; Mass: Actual: 377 m/z; Found: 377 m/z.

##### 5.4.2.4. (Z)-5-bromo-2-(4-((3-chloro-1,2,3,4-tetrahydroquinoxalin-2-yl)amino)styryl)phenol (M5)

$\text{C}_{22}\text{H}_{19}\text{BrClN}_3\text{O}$ ; Pale white solid; MP: 119 – 121 $^{\circ}\text{C}$ ; Rf: 0.59; IR (KBr)  $\text{cm}^{-1}$ : 3510 (OH str); 3464 (NH str, Amine) 3098 (CH str alkene); 2986 (CH str alkane); 2200 (CH str aromatic); 1435 (CN bending); 970 (Aromatic ring); 730 (C-Br str);  $^1\text{H}$  NMR (500 MHz, DMSO)  $\delta$  9.91 (s, 1H), 9.88 (s, 2H), 9.69 (s, 4H), 7.00 (td,  $J = 7.5, 1.4$  Hz, 1H), 6.86 (td,  $J = 7.5, 1.6$  Hz, 2H), 6.78 (dd,  $J = 7.5, 1.5$  Hz, 1H), 6.58 – 6.45 (m, 1H),

6.42 – 6.28 (m, 1H), 5.80 (s, 2H), 5.56 (s, 1H), 4.99 (d, J = 7.9 Hz, 1H), 4.83 (d, J = 7.9 Hz, 1H). <sup>13</sup>C NMR (126 MHz, DMSO): δ 170.45, 168.50, 156.63, 151.43, 148.92, 148.39, 144.58, 142.03, 140.01, 138.30, 138.08, 136.06, 131.82, 130.92, 127.79, 126.96, 125.64, 125.25, 123.83, 123.01, 121.60; Mass: Actual: 455 m/z; Found: 457 (M+2) m/z.

#### 5.4.2.5.(Z)-4-bromo-2-(4-((3-chloro-1,2,3,4-tetrahydroquinoxalin-2-yl)amino)styryl)phenol (M6)

C<sub>22</sub>H<sub>19</sub>BrClN<sub>3</sub>O; Pale white solid; MP: 118 – 121°C; Rf: 0.58; IR (KBr) cm<sup>-1</sup>: 3510 (OH str); 3324 (NH str, Amine) 3074 (CH str alkene); 2937 (CH str alkane); 2604 (CH str aromatic); 1403 (CN bending); 950 (Aromatic ring); 720 (C-Clstr); <sup>1</sup>H NMR (500 MHz, DMSO) δ 9.91 (s, 1H), 9.88 (s, 2H), 9.69 (s, 4H), 7.00 (td, J = 7.5, 1.4 Hz, 1H), 6.86 (td, J = 7.5, 1.6 Hz, 2H), 6.78 (dd, J = 7.5, 1.5 Hz, 1H), 6.58 – 6.45 (m, 1H), 6.42 – 6.28 (m, 1H), 5.80 (s, 2H), 5.56 (s, 1H), 4.99 (d, J = 7.9 Hz, 1H), 4.83 (d, J = 7.9 Hz, 1H); <sup>13</sup>C NMR (126 MHz, DMSO) δ: 170.45, 168.50, 156.63, 151.43, 148.92, 148.39, 144.58, 142.03, 140.01, 138.30, 138.08, 136.06, 131.82, 130.92, 127.79, 126.96, 125.64, 125.25, 123.83, 123.01, 121.60; Mass: Actual: 455 m/z; Found: 456 (M+1).

#### 5.4.2.6.(Z)-3-chloro-N-(4-(4-methylstyryl)phenyl)-1,2,3,4-tetrahydroquinoxalin-2-amine (M7)

C<sub>23</sub>H<sub>22</sub>ClN<sub>3</sub>; White solid; MP: 116 – 118°C; Rf: 0.69; IR (KBr) cm<sup>-1</sup>: 3467 (NH str, Amine) 2884 (CH str alkane); 2641 (CH str aromatic); 1403 (CN bending); 951 (Aromatic ring); 740 (C-Clstr); <sup>1</sup>H NMR (500 MHz, DMSO) δ 9.77 (s, 1H), 9.72 (s, 1H), 8.35 (s, 2H), 7.25 (d, J = 7.5 Hz, 2H), 7.16 (d, J = 7.5 Hz, 2H), 6.58 – 6.28 (m, 2H), 5.81 (s, 1H), 5.56 (s, 1H), 4.99 (d, J = 7.9 Hz, 1H), 4.83 (d, J = 7.9 Hz, 1H), 2.35 (s, 3H); <sup>13</sup>C NMR (126 MHz, DMSO) δ: 170.45, 168.50, 156.63, 151.43, 148.92, 148.39, 144.58, 142.03, 140.01, 138.30, 138.08, 136.06, 131.82, 130.92, 127.79, 126.96, 125.64, 125.25, 123.83, 123.01, 121.60; Mass: Actual: 375 m/z; Found: 375 m/z.

#### 5.4.2.7.(Z)-3-chloro-N-(4-(4-methoxystyryl)phenyl)-1,2,3,4-tetrahydroquinoxalin-2-amine (M8)

C<sub>23</sub>H<sub>22</sub>ClN<sub>3</sub>O; White solid; MP: 124 – 127°C; Rf: 0.67; IR (KBr) cm<sup>-1</sup>: 3476 (NH str, Amine) 3017 (CH str alkene); 2960 (CH str alkane); 2741 (CH str aromatic); 1406 (CN bending); 902 (Aromatic ring); 800 (C-Clstr); ; <sup>1</sup>H NMR (500 MHz, DMSO) δ 9.82 (d, J = 0.5 Hz, 2H), 7.41 (d, J = 7.5 Hz, 3H), 7.29 – 7.21 (m, 1H), 6.90 (d, J = 7.5 Hz, 1H), 6.57 – 6.28 (m, 1H), 5.81 (s, 1H), 5.57 (s, 1H), 4.99 (d, J = 7.9 Hz, 1H), 4.83 (d, J = 7.9 Hz, 1H), 3.81 (s, 3H); <sup>13</sup>C NMR (126 MHz, DMSO): δ 170.30, 167.02, 155.81, 154.37, 134.50, 134.05, 132.33, 131.51, 130.09, 129.99, 129.50, 129.31, 129.20, 128.68, 128.07, 128.03, 127.79, 127.03, 124.95, 124.45, 119.01; Mass: Actual: 391 m/z; Found: 392 (M-1) m/z.

#### 5.4.2.8.(Z)-N-(4-(2-(1H-imidazol-2-yl)vinyl)phenyl)-3-chloro-1,2,3,4-tetrahydroquinoxalin-2-amine (M13)

C<sub>19</sub>H<sub>18</sub>ClN<sub>5</sub>; Pale brown solid; MP: 122 – 125°C; Rf: 0.62; IR (KBr) cm<sup>-1</sup>: 3420 (NH str, Amine) 3041 (CH str alkene); 2960 (CH str alkane); 2684 (CH str aromatic); 1400 (CN bending); 948 (Aromatic ring); 750 (C-Clstr); ; <sup>1</sup>H NMR (500 MHz, DMSO) δ 7.18 (d, J = 7.5 Hz, 2H), 7.03 (d, J = 7.3 Hz, 1H), 6.97 (d, J = 7.5 Hz, 1H), 6.58 (dd, J = 20.5, 9.1 Hz, 3H), 6.52 – 6.42 (m, 3H), 6.38 – 6.25 (m, 3H), 5.70 (s, 1H), 5.57 (s, 1H), 4.99 (d, J = 7.9 Hz, 1H), 4.83 (d, J = 7.9 Hz, 1H), 4.53 (s, 1H). <sup>13</sup>C NMR (126 MHz, DMSO) δ 173.30, 156.00, 154.28, 147.72, 142.88, 140.34, 137.80, 136.37, 135.78, 135.48, 133.55, 132.13, 131.99, 131.83, 129.79, 128.41, 127.66, 127.05, 126.64, 124.97, 124.26, 118.52; Mass: Actual: 351 m/z; Found: 352 (M+1).

#### 5.4.2.9.(Z)-3-chloro-N-(4-(4-(dimethylamino)styryl)phenyl)-1,2,3,4-tetrahydroquinoxalin-2-amine (M14)

C<sub>24</sub>H<sub>25</sub>ClN<sub>4</sub>; Red solid; MP: 123 – 125°C; Rf: 0.66; IR (KBr) cm<sup>-1</sup>: 3393 (NH str, Amine) 3042 (CH str alkene); 2937 (CH str alkane); 2641 (CH str aromatic); 1403 (CN bending); 951 (Aromatic ring); 740 (C-Clstr); <sup>1</sup>H NMR (500 MHz, DMSO) δ 7.30 – 7.21 (m, 5H), 6.71 – 6.56 (m, 2H), 6.56 – 6.33 (m, 8H), 5.81 (s, 1H), 5.56 (s, 1H), 4.99 (s, 1H), 4.83 (s, 1H), 2.95 – 2.91 (m, 6H); <sup>13</sup>C NMR (126 MHz, DMSO) δ 173.30, 156.00, 154.28, 147.72, 142.88, 140.34, 137.80, 136.37, 135.78, 135.48, 133.55, 132.13, 131.99, 131.83, 129.79, 128.41, 127.66, 127.05, 126.64, 124.97, 124.26, 118.52; Mass: Actual: 404 m/z; Found: 405 (M+1).

#### 5.4.2.10.(Z)-3-chloro-N-(4-(4-nitrostyryl)phenyl)-1,2,3,4-tetrahydroquinoxalin-2-amine (M15)

C<sub>22</sub>H<sub>19</sub>ClN<sub>4</sub>O<sub>2</sub>; Yellow solid; MP: 123 – 125°C; Rf: 0.66; IR (KBr) cm<sup>-1</sup>: 3524 (NH str, Amine) 3162 (CH str alkene); 2912 (CH str alkane); 2741 (CH str aromatic); 1430 (CN bending); 905 (Aromatic ring); 720 (C-Clstr); <sup>1</sup>H NMR (500 MHz, DMSO) δ 8.04 – 7.89 (m, 2H), 7.71 – 7.57 (m, 2H), 7.33 – 7.18 (m, 3H), 6.64 (s, 1H), 6.54 – 6.48 (m, 3H), 6.38 (dd, J = 26.9, 0.8 Hz, 4H), 5.80 (s, 1H), 5.56 (s, 1H), 4.99 (s, 1H), 4.83 (s, 1H). <sup>13</sup>C NMR (126 MHz, DMSO) δ 167.31, 149.52, 149.42, 148.31, 147.69, 140.02, 135.16, 133.23, 130.74, 130.46, 129.50, 128.98, 128.08, 126.66, 125.84, 124.95, 124.56, 124.43, 124.30, 124.18, 122.98, 121.93, 121.86; Mass: Actual: 406 m/z; Found: 406 m/z.

### 2.5MTT assay for cell viability

The MTT test was utilized to gauge cell viability. The cells were plated in a 96-well plate with 1 10<sup>4</sup> cells per well which were determined by reading the control and plotting a logarithmic graph of the percentage of cell viability Vs sample concentration. Averaging the results of the triple trials allowed for the determination of the final concentration that yields the maximum viability. For the *in vitro* cytotoxicity examination, the MTT assay method was applied to human SH-SY5Y neuroblastoma cells. All of the medications under investigation have improved survival of more than 70% at concentration 500nm. Among the tested compounds, the derivative M2 substituted with highly electronegative atom Cl shows promising viability 79.62% at the concentration range 500 nm, followed by the compound M4 substituted with electronegative atoms like OH and Cl atom shows good percentage viability 78.37% at 500 nm, against the tested cell line Human SH-SY5Y neuroblastoma. Based on the results it's clearly showed that, the electronegative atom may alter the biological activity of the compounds in tested cell lines.

**Table 4.** Results for *in vitro* MTT assay of cell viability of the compounds

Compound	% viability
M2	79.62
M3	75.25
M4	78.37
M5	69.41
M6	75.66
M7	66.29
M8	73.72
M13	76.61
M14	71.29
M15	77.62

## 4. CONCLUSION

The structure of the newly synthesized compounds was validated by physical, chemical, and spectroscopic data. In molecular docking studies, the studied drugs demonstrated a similar mechanism of protein binding to the active region of the acetyl cholinesterase protein (PDB ID:4EY6). According on the predicted docking energies, the interaction with *cholinesterase* enzyme is shows promising binding energy. All substances were tested for viability *in vitro* against Human SH-SY5Y neuroblastoma cell lines. Compounds M2 and M4 were shown to be the most effective against the evaluated cell lines. Work is being done to advance the search for new *cholinesterase* inhibitors. In order to establish a SAR for rational study, more derivatives and in-depth, detailed investigations on *in vivo* activity may be undertaken. The current study suggests that more research is needed for chalcone merged quinoxaline derivatives developed as a potent lead for Alzheimer's disease.

### ACKNOWLEDGEMENT:

A major thanks to the department of pharmaceutical chemistry people who supported during this research.

**CONFLICT OF INTEREST:** The author has no conflict of interest.

### REFERENCES

1. Viegas-Junior, C.; Danuello, A.; da Silva Bolzani, V.; Barreiro, E. J.; Fraga, C. A. M. Molecular hybridization: a useful tool in the design of new drug prototypes. *Curr. Med. Chem.* 2007, 14, 1829–1852.
2. Zhan, P.; Liu, X. Y. Designed Multiple Ligands: An Emerging Anti-HIV Drug Discovery Paradigm. *Curr. Pharm. Des.* 2009, 15, 1893–1917.
3. Zhuang, C. L.; Miao, Z. Y.; Wu, Y. L.; Guo, Z. Z.; Li, J.; Yao, J. Z.; Xing, C. G.; Sheng, C. Q.; Zhang, W. N. Double-Edged Swords as Cancer Therapeutics: Novel, Orally Active, Small Molecules Simultaneously Inhibit p53-MDM2 Interaction and the NF-kappa B Pathway. *J. Med. Chem.* 2014, 57, 567–577.

4. Viegas-Junior C, Danuello A, da Silva Bolzani V, Barreiro EJ, Fraga CA. Molecular hybridization: a useful tool in the design of new drug prototypes. *Current medicinal chemistry*. 2007 Jul 1;14(17):1829-52.
5. Lazar C, Kluczyk A, Kiyota T, Konishi Y. Drug evolution concept in drug design: 1. Hybridization method. *Journal of medicinal chemistry*. 2004 Dec 30;47(27):6973-82.
6. Zhou, B.; Xing, C. Diverse Molecular Targets for Chalcones with Varied Bioactivities. *Med. Chem.* 2015, 5, 388–404.
7. Batovska, D. I.; Todorova, I. T. Trends in utilization of the pharmacological potential of chalcones. *Curr. Clin. Pharmacol.* 2010, 5, 1–29.
8. Sahu, N. K.; Balbhadra, S. S.; Choudhary, J.; Kohli, D. V. Exploring pharmacological significance of chalcone scaffold: a review. *Curr. Med. Chem.* 2012, 19, 209–225.
9. Singh, P.; Anand, A.; Kumar, V. Recent developments in biological activities of chalcones: a mini review. *Eur. J. Med. Chem.* 2014, 85, 758–777.
10. Karthikeyan, C.; Moorthy, N. S.; Ramasamy, S.; Vanam, U.; Manivannan, E.; Karunakaran, D.; Trivedi, P. Advances in Chalcones with anticancer activities. *Recent Pat. Anti-Cancer Drug Discovery* 2015, 10, 97–115.
11. Sebti, S.; Solhy, A.; Smahi, A.; Kossir, A.; Oumimoun, H. Dramatic activity enhancement of natural phosphate catalyst by lithium nitrate. An efficient synthesis of chalcones. *Catal. Commun.* 2002, 3, 335–339.
12. Sharma, V.; Kumar, V.; Kumar, P. Heterocyclic Chalcone analogues as potential anticancer agents. *Anti-Cancer Agents Med. Chem.* 2013, 13, 422–432.
13. Dimmock, J. R.; Elias, D. W.; Beazely, M. A.; Kandepu, N. M. Bioactivities of chalcones. *Curr. Med. Chem.* 1999, 6, 1125–1149.
14. Go, M. L.; Wu, X.; Liu, X. L. Chalcones: an update on cytotoxic and chemoprotective properties. *Curr. Med. Chem.* 2005, 12, 483–499.
15. Leon-Gonzalez, A. J.; Acero, N.; Munoz-Mingarro, D.; Navarro, I.; Martin-Cordero, C. Chalcones as Promising Lead Compounds on Cancer Therapy. *Curr. Med. Chem.* 2015, 22, 3407–3425.
16. Mahapatra, D. K.; Asati, V.; Bharti, S. K. Chalcones and their therapeutic targets for the management of diabetes: structural and pharmacological perspectives. *Eur. J. Med. Chem.* 2015, 92, 839–865.
17. Mahapatra, D. K.; Bharti, S. K.; Asati, V. Chalcone scaffolds as anti-infective agents: structural and molecular target perspectives. *Eur. J. Med. Chem.* 2015, 101, 496–524.
18. Mahapatra, D. K.; Bharti, S. K.; Asati, V. Anti-cancer chalcones: Structural and molecular target perspectives. *Eur. J. Med. Chem.* 2015, 98, 69–114.
19. Kamal, A.; Kashi Reddy, M.; Viswanath, A. The design and development of imidazothiazole-chalcone derivatives as potential anticancer drugs. *Expert Opin. Drug Discovery* 2013, 8, 289–304.
20. Matos, M. J.; Vazquez-Rodriguez, S.; Uriarte, E.; Santana, L. Potential pharmacological uses of chalcones: a patent review (from June 2011 - 2014). *Expert Opin. Ther. Pat.* 2015, 25, 351–366.
21. Das, M.; Manna, K. Chalcone Scaffold in Anticancer Armamentarium: A Molecular Insight. *J. Toxicol.* 2016, 2016, 7651047.
22. Mahapatra, D. K.; Bharti, S. K. Therapeutic potential of chalcones as cardiovascular agents. *Life Sci.* 2016, 148, 154–172.
23. Bukhari, S. N.; Franzblau, S. G.; Jantan, I.; Jasamai, M. Current prospects of synthetic curcumin analogs and chalcone derivatives against mycobacterium tuberculosis. *Med. Chem.* 2013, 9, 897–903.
24. Nasir Abbas Bukhari, S. N.; Jasamai, M.; Jantan, I. Synthesis and biological evaluation of chalcone derivatives (mini review). *Mini-Rev. Med. Chem.* 2012, 12, 1394–1403.
25. Kontogiorgis, C.; Mantzanidou, M.; Hadjipavlou-Litina, D. Chalcones and their potential role in inflammation. *Mini-Rev. Med. Chem.* 2008, 8, 1224–1242.
26. Kumar, D, Kumar M, Kumar A; Singh, S. K. Chalcone and curcumin derivatives: a way ahead for malarial treatment. *Mini-Rev. Med. Chem.* 2013, 13, 2116–2133.
27. Shagufta; Ahmad, I. An insight into the therapeutic potential of quinazoline derivatives as anticancer agents. *Med. Chem. Com.* 2017, 8, 871–885.
28. Shagufta; Ahmad, I. Recent insight into the biological activities of the synthetic xanthone derivatives. *Eur. J. Med. Chem.* 2016, 116, 267–280.
29. Ahmad, I.; Shagufta. Recent developments in steroidal and nonsteroidal aromatase inhibitors for the chemoprevention of oestrogen-dependent breast cancer. *Eur. J. Med. Chem.* 2015, 102, 375–386.
30. Ahmad, I.; Shagufta, S. An important class of organic compounds with diverse biological activities. *Int. J. Pharm. Sci.* 2015, 7, 19–27.

31. G.W.H. Chessemann, R.F. C., The Chemistry of Heterocyclic Compounds, Condensed Pyrazines, vol. 35, John Wiley & Sons, Inc., 1979.
32. A. Patidar, J. M., A. Mobiya, G. Selvam, Int. J. PharmTech Res. 3 (2011) 386e392.
33. A.s. Association, 2020 Alzheimer's disease facts and figures, Alzheimers Dement, 2020.
34. H. Hippus, G. Neundorfer, The discovery of Alzheimer's disease, Dialog. Clin. Neurosci. 5 (2003) 101–108.
35. W.V. Graham, A. Bonito-Oliva, T.P. Sakmar, Update on Alzheimer's Disease Therapy and Prevention Strategies, Annu. Rev. Med. 68 (2017) 413–430.
36. S.L. Rogers, R.S. Doody, R.C. Mohs, L.T. Friedhoff, Donepezil improves cognition and global function in Alzheimer disease: a 15-week, double-blind, placebo-controlled study. Donepezil Study Group, Arch. Intern. Med. 158 (1998) 1021–1031.
37. H. Sugimoto, Donepezil hydrochloride: a treatment drug for Alzheimer's disease, Chem. Rec. 1 (2001) 63–73.
38. H. Sugimoto, H. Ogura, Y. Arai, Y. Limura, Y. Yamanishi, Research and development of donepezil hydrochloride, a new type of *acetylcholinesterase* inhibitor, Jpn. J. Pharmacol. 89 (2002) 7–20.
39. G.T. Grossberg, C. Sadowsky, J.T. Olin, Rivastigmine transdermal system for the treatment of mild to moderate Alzheimer's disease, Int. J. Clin. Pract. 64 (2010) 651–660.
40. K. Articus, M. Baier, F. Tracik, F. Kuhn, U.W. Preuss, A. Kurz, A 24-week, multicentre, open evaluation of the clinical effectiveness of the rivastigmine patch in patients with probable Alzheimer's disease, Int. J. Clin. Pract. 65 (2011) 790–796.
41. R. Khoury, J. Rajamanickam, G.T. Grossberg, An update on the safety of current therapies for Alzheimer's disease: focus on rivastigmine, Ther. Adv. Drug Saf. 9 (2018) 171–178.
42. D. Prvulovic, H. Hampel, J. Pantel, Galantamine for Alzheimer's disease, Expert Opin. Drug Metab. Toxicol. 6 (2010) 345–354.
43. M.A. Raskind, Update on Alzheimer drugs (galantamine), Neurologist 9 (2003) 235–240.
44. S. Matsunaga, T. Kishi, I. Nomura, K. Sakuma, M. Okuya, T. Ikuta, N. Iwata, The efficacy and safety of memantine for the treatment of Alzheimer's disease, Expert Opin. Drug Saf. 17 (2018) 1053–1061.
45. D. Galimberti, E. Scarpini, Old and new *acetylcholinesterase* inhibitors for Alzheimer's disease, Expert Opin. Invest. Drugs 25 (2016) 1181–1187.
46. R.T. Bartus, R.L. Dean, B. Beer, A.S. Lipka, The cholinergic hypothesis of geriatric memory dysfunction, Science 217 (1982) 408–414.
47. P. Davies, A.J. Maloney, Selective loss of central cholinergic neurons in Alzheimer's disease, Lancet 2 (1976) 1403.
48. D. Wu, L.B. Hersh, Choline acetyltransferase: celebrating its fiftieth year, J. Neurochem. 62 (1994) 1653–1663.
49. T.H. Ferreira-Vieira, I.M. Guimaraes, F.R. Silva, F.M. Ribeiro, Alzheimer's disease: Targeting the Cholinergic System, Curr. Neuropharmacol. 14 (2016) 101–115.
50. P. Taylor, Z. Radic, The *cholinesterases*: from genes to proteins, Annu. Rev. Pharmacol. Toxicol. 34 (1994) 281–320.
51. P. Guyenet, P. Lefresne, J. Rossier, J.C. Beaujouan, J. Glowinski, Inhibition by hemicholinium-3 of (14C)acetylcholine synthesis and (3H)choline high-affinity uptake in rat striatal synaptosomes, Mol. Pharmacol. 9 (1973) 630–639.
52. A. Rampa, S. Montanari, L. Pruccoli, M. Bartolini, F. Falchi, A. Feoli, A. Cavalli, F. Belluti, S. Gobbi, A. Tarozzi, A. Bisi, Chalcone-based carbamates for Alzheimer's disease treatment, Future Med. Chem. 9 (2017) 749–764.
53. G. Xiao, Y. Li, X. Qiang, R. Xu, Y. Zheng, Z. Cao, L. Luo, X. Yang, Z. Sang, F. Su, Y. Deng, Design, synthesis and biological evaluation of 4'-aminochalcone-rivastigmine hybrids as multifunctional agents for the treatment of Alzheimer's disease, Bioorg. Med. Chem. 25 (2017) 1030–1041.
54. H.R. Liu, X.J. Liu, H.Q. Fan, J.J. Tang, X.H. Gao, W.K. Liu, Design, synthesis and pharmacological evaluation of chalcone derivatives as *acetylcholinesterase* inhibitors, Bioorg. Med. Chem. 22 (2014) 6124–6133.
55. H.R. Liu, C. Zhou, H.Q. Fan, J.J. Tang, L.B. Liu, X.H. Gao, Q.A. Wang, W.K. Liu, Novel Potent and Selective *Acetylcholinesterase* Inhibitors as Potential Drugs for the Treatment of Alzheimer's Disease: Synthesis, Pharmacological Evaluation, and Molecular Modeling of Amino-Alkyl-Substituted Fluoro-Chalcones Derivatives, Chem. Biol. Drug Des. 86 (2015) 517–522.
56. X.H. Gao, C. Zhou, H.R. Liu, L.B. Liu, J.J. Tang, X.H. Xia, Tertiary amine derivatives of chlorochalcone as *acetylcholinesterase* (AChE) and buthylcholinesterase (BuChE) inhibitors: the influence of chlorine,

- alkyl amine side chain and alpha, beta-unsaturated ketone group, *J. Enzyme Inhib. Med. Chem.* 32 (2017) 146–152.
- 57.L. Huang, H. Miao, Y. Sun, F. Meng, X. Li, Discovery of indanone derivatives as multi-target-directed ligands against Alzheimer's disease, *Eur. J. Med. Chem.* 87 (2014) 429–439.
- 58.C.B. Mishra, S. Kumari, A. Manral, A. Prakash, V. Saini, A.M. Lynn, M. Tiwari, Design, synthesis, *in-silico* and biological evaluation of novel donepezil derivatives as multi-target-directed ligands for the treatment of Alzheimer's disease, *Eur. J. Med. Chem.* 125 (2017) 736–750.
- 59.Sukumaran SD, Chee CF, Viswanathan G, *et al.* Synthesis, biological evaluation and molecular modelling of 2'-hydroxychalcones as *acetylcholinesterase* inhibitors. *Molecules* 2016; 21(7): 955.
- 60.Rampa A, Bartolini M, Prucoli L, *et al.* Exploiting the chalcone scaffold to develop multifunctional agents for Alzheimer's disease. *Molecules* 2018; 23(8): 1902.
- 61.Sagar SR, Singh DP, Das RD, Panchal NB, Sudarsanam V, Nivsarkar M, Vasu KK. Pharmacological investigation of quinoxaline-bisthiazoles as multitarget-directed ligands for the treatment of Alzheimer's disease. *Bioorganic chemistry*. 2019 Aug 1;89:102992.
- 62.Kanhed AM, Patel DV, Patel NR, Sinha A, Thakor PS, Patel KB, Prajapati NK, Patel KV, Yadav MR. Indoloquinoxaline derivatives as promising multi-functional anti-Alzheimer agents. *Journal of Biomolecular Structure and Dynamics*. 2020 Oct 27:1-8.

Mahajan S, Slathia N, Nuthakki VK, Bharate SB, Kapoor KK. Malononitrile-activated synthesis and *anti-cholinesterase* activity of styrylquinoxalin-2 (1 H)-ones. *RSC Advances*. 2020;10(27):15966-75.